ASAP 7 – ACAP Final Report

Austrian Space Application Program

Global Gravity Field Modelling from Orbit Data based on the Acceleration Approach
ACAP

Final Report

Graz University of Technology
Institute of Theoretical Geodesy and Satellite Geodesy (ITSG)
October 2012

bmvit
Austrian Ministry for Transport, Innovation and Technology
>asap>
FFG

Abstract

In the past few years some satellite missions dedicated to the study of Earth's gravity field have been realized. Since then gravity field related observations and precise orbit information are available. To derive gravity field models from orbit information numerous approaches exist.
In this project the focus lies on the acceleration approach. It is based on Newton's second law of motion which states that the accelerations of a body are directly related to the forces acting on this body or in this case to the gradients of the gravitational potential. Therefore the key issue is the numerical differentiation of the satellite positions to derive the required accelerations. For this purpose the Taylor-MacLaurin method, the Newton-Gregory interpolation and the polynomial interpolation were investigated.
The studies showed that in fact the Taylor-MacLaurin and the Newton-Gregory methods can be reduced to a simple polynomial interpolation. Therefore they provide no benefits. Additionally the numeric stability of the interpolation was investigated and an optimal implementation found. Based on this implementation different kinds of polynomials were tested. The conclusion is that the degree of the polynomial has no effect on the accuracy. Also an overdetermination has only a small positive effect but when it gets too big the solution is destroyed.
Based on the findings from the mentioned investigations, real satellite data has been used to produce different gravity field solutions. Orbit information from two different satellite missions, CHAMP and GOCE, was available for this project. These data sets were used to produce a gravity field solution for each satellite separately and a combined solution. All three different models are compared to current state-of-the-art models, like for example GOCO02S. These comparisons showed that the acceleration approach is capable of producing results with the same quality as for example the celestial mechanics approach or the short arc integral method. It also showed that the acceleration approach is superior to the energy balance approach.
All in all it can be said, that the implemented software works correctly. It has been tested intensively and the produced gravity field estimates reach the expected quality.

Kurzfassung

In den letzten Jahren wurden mehrere Satellitenmissionen zur Untersuchung des Schwerefeldes der Erde gestartet. Diese liefern präzise Beobachtungen und Orbitinformationen. Um aus den Orbitinformationen ein Schwerefeld abzuleiten gibt es mehrere Ansätze.
In diesem Projekt liegt der Fokus auf dem Beschleunigungsansatz. Er basiert auf dem zweiten newtonschen Gesetz, wonach die Beschleunigung eines Körpers direkt von den wirkenden Kräften abhängig ist, in diesem Fall der Gradient des Gravitationspotentials. Deshalb ist der wichtigste Schritt die nummerische Differentiation um die benötigten Beschleunigungen aus den Positionen zu berechnen. Zu diesem Zweck wurden die

Taylor-MacLaurin Methode, die Newton-Gregory Interpolation und die Polynominterpolation untersucht.
Die Untersuchungen haben gezeigt, dass sowohl Taylor-MacLaurin als auch Newton-Gregory auf die Polynominterpolation zurückzuführen sind. Diese Methoden bieten daher auch keine Vorteile. Zusätzlich wurde noch die numerische Stabilität der Polynominterpolation untersucht und eine optimale Umsetzung gefunden. Basierend auf der gefundenen Implementierung wurden unterschiedliche Polynome untersucht. Dies hat gezeigt, dass der Grad des Polynoms keinen und das Ausmaß der Überbestimmung nur einen geringen positiven Einfluss auf die Qualität der Ergebnisse hat. Wird die Überbestimmung jedoch zu groß so wird die Lösung zerstört.
Basierend auf den Ergebnissen der erwähnten Untersuchungen wurden Echtdaten der beiden Satellitenmissionen, CHAMP und GOCE, verwendet um unterschiedliche Schwerefeldlösungen zu produzieren. Es wurde jeweils ein Schwerefeld aus den Daten der einzelnen Satelliten gerechnet und anschließend wurden die Daten gemeinsam verarbeitet um eine kombinierte Lösung zu generieren. Alle drei gerechneten Lösungen wurden mit aktuellen Schwerefeldlösungen, wie beispielsweise dem GOCO02S verglichen. Diese Vergleiche haben gezeigt, dass der implementierte Beschleunigungsansatz in der Lage ist gleichwertige Lösungen zu liefern, wie etwa der celestial mechanics approach oder die short arc integral methode. Es hat sich auch gezeigt, dass der Beschleunigungsansatz bessere Ergebnisse liefert als der Energieerhaltungsansatz.
Im Gesamten betrachtet kann gesagt werden, dass die erstellte Software korrekte Ergebnisse liefert. Sie wurde intensiv getestet und die bisher damit erzeugten Schwerefeldlösungen weisen die zu erwartende Qualität auf.

Table of Contents

1 Introduction

1.1 Motivation

During the last decade three satellites for studying the Earth's gravity field have been constructed. The satellites CHAMP, GRACE and GOCE were launched in the years 2000, 2002 and 2009. In contrast to former methods of terrestrial or airborne gravity observations these satellites deliver homogeneous, globally distributed and continuous gravity observations and orbit information.
Numerous approaches exist for deriving gravity field models from the observations. The different approaches are based on observations of instruments on board the satellite or on the precise orbit positions. The most important methods which use the orbit information are the variational equations approach, the short arc integral approach, the energy balance approach and the acceleration approach. The Institute for Theoretical Geodesy and Satellite Geodesy (ITSG), respectively the according part of the former Institute for Navigation and Satellite Geodesy (INAS), has already successfully implemented the energy balance approach in the frame of previous projects and is using the produced software for generating gravity field models based on GOCE data. Now the acceleration approach will be implemented, investigated and used.

1.2 Executive Summary

In this project the focus lies on implementing and testing the acceleration approach. It is based on Newton's second law of motion which states that the accelerations of a body are directly related to the forces acting on this body. Transferred to satellite based gravity field determination this law means that the accelerations derived from the orbit positions are directly related to the gradients of the gravitational potential.
The most important advantage of the acceleration approach compared to the energy balance approach is the fact that full 3D information can be used. Three accelerations, one for every coordinate direction can be computed at every epoch. The kinetic energy on the other hand is one scalar value for every epoch. Due to this fact, the acceleration approach achieves a higher redundancy than the energy balance approach does, which in turn results in a better estimation of the geopotential coefficients.
The key issue for the acceleration approach is the numerical differentiation of the satellite positions to derive the required accelerations. Therefore a suitable differentiation method has to be used and first of all found. Various methods have been used until now. At the ITSG the Taylor-MacLaurin method is already in use to derive the velocities for the energy balance approach and has proved to be a powerful tool in terms of numerical differenti-

ation and attenuation of high frequencies at the same time. Additionally other methods, like Newton-Gregory interpolation or polynomial interpolation were investigated.
The studies were carried out by means of closed-loop simulations. First of all the different differentiation methods were compared to each other. These investigations revealed that the special methods like Taylor-MacLaurin and Newton-Gregory can be represented by a simple polynomial interpolation. Therefore these methods have no advantage compared to the polynomial interpolation. Additionally the polynomial interpolation provides more flexibility in terms of changing the desired properties of the computation. Afterwards the implementation was tested regarding numeric stability.
After testing the software, different realizations of the differentiator were investigated with respect to the impact on the produced gravity field solutions. The studies showed that on the one hand the degree of the used polynomial has no effect on the accuracy of the solution and the used overdetermination only has a small positive effect. But on the other hand, if the overdetermination gets to big, it destroys the accuracy of the derived gravity field model. Due to these facts the best differentiator is a polynomial with a degree of about 6 to 10 with no overdetermination. This has the effect that not too much data points are lost due to the filter process and these degrees keep the possibility of numeric instability low.
After intensive testing of the implemented software the acceleration approach is applied to real satellite data. For this purpose data from two different satellite missions was used. The two missions are the CHAMP and GOCE satellites flying in a low earth orbit dedicated to studying the Earth's gravity field. The datasets of orbit information and additional observations like attitude and non-conservative accelerations spans a time frame from 2002 till 2009 for CHAMP and from November 2009 till July 2011 for GOCE. Based on these data sets two separate gravity field solutions are produced. Both solutions suffer from different drawbacks of the specific satellite mission. A third solution was generated incorporating both data sets, which improves the solution due to the bigger amount of data. But it also eliminates the influence of certain drawbacks, like for example the polar gap issue in case of the GOCE satellite.
The three gravity field models were validated against state-of-the-art models like for example GOCO02S [11] or EGM2008 [24]. These investigations showed that the implemented software and therefore the acceleration approach itself is capable of producing high quality gravity field solutions based on orbit positions. This means the acceleration approach produces comparable results as the celestial mechanics approach or the short arc integral method. It also turned out that it is superior to the energy balance approach.
Therefore it can be said that the implemented software works correct and produces high quality gravity field estimates. The software itself is integrated in an existing software package which is based on object oriented programming and therefore is flexible for future developments. At the current state the implemented module for the acceleration approach is tested and ready for further real data applications or future projects at the ITSG.

2 WP 0 - Scientific and administrative management

2.1 Experiences of contractor

The former Institute of Navigation and Satellite Geodesy (INAS) was split into the Institute of Navigation and the Institute of Theoretical Geodesy and Satellite Geodesy (ITSG). In the past decades the INAS now followed by the ITSG has gained a reasonable experience in satellite geodesy and especially in gravity field determination. The contractor of this project has been part of many projects concerning gravity field determination in all aspects such as

- ESA studies CIGAR II, III and IV (ESA, 1989, [6], ESA, 1993, [8], ESA, 1995, [7], ESA, 1996)
- From Eötvös to mGal (Sünkel, 2000, [27])
- From Eötvös to mGal+ (Sünkel,2002, [26])
- GOCE: Preparation of the GOCE Level 1 to Level 2 Data Processing (Koop and Sünkel, 2002, [16])
- Data Archiving and Processing centre (DAPC) Graz, Phase Ia (Pail, 2003, [22]) and Bridging Phase (Pail, 2004, [21]): ASAP Phase I project
- GOCE High-level Processing Facility (HPF) (EGG-C (2004), Rummel et al. (2004), Pail et al. (2007)): ESA project
- Gravity Field Processing Facility (GFPF) Graz (Pail, 2006, [20]): ASAP Phase II project
- The Austrian Geoid 2007 (GEOnAUT) (Pail, 2007, [19]): ASAP Phase III project
- Improved kHz-SLR Tracking Techniques and Orbit Quality Analysis for LEO Missions (LEO-SLR) (Hausleitner et al. 2010, [12]): ASAP Phase III project
- Development of a processing facility for the purpose of modeling snow and ice masses in polar regions, based on a combination of terrestrial satellite data (ICEAGE) (Heuberger et al. 2010, [23]) : ASAP Phase V project
- Combined high-resolution global gravity field model from satellite gravity missions GOCE, GRACE and CHAMP, completed by terrestrial gravity, altimetry and SLR data (GOCOnAUT): ASAP Phase VI project

2.2 Scope of this project

The objective of the present project was to implement the so called acceleration approach for gravity field determination. The focus lied on investigation of different types of numeric differentiators concerning their advantages and disadvantages. This was done on different levels. First of all the different types were compared to each other only on analytical basis. Then a comparison by means of the numerical values of the differentiation operators was conducted. Especially the individual behavior of the differentiators in the frequency domain was of particular interest. Next step was to investigate the quality of derived accelerations and finally derived gravity field models were compared to each other and to other published models.
After these examinations a global gravity field model was computed incorporating the differentiator which performed best in the previously mentioned investigations.

The present project addressed the following core tasks:

- Improvement of the scientific significance and standing in the international research environment and supporting scientific excellence
- Enlargement of the scientific fundamentals
- Acquisition of new know-how in fundamental research

Based on the available knowledge at the ITSG this project aimed at producing a gravity field model with high accuracy. This will attract attention and further strengthen the reputation of the Institute in the international research community.

In the “Proposal: Global Gravity Field Modeling from Orbit Data based on the Acceleration Approach – ACAP” (Goiginger et. al., 2010, [10]) the following work packages have been proposed:

WP	Description
0	**Scientific and administrative management**
1	**Processing of satellite accelerations** Development and implementation of algorithms, outlier detection and data gap handling, derivation of accelerations based on orbit data
2	**Numerical studies** Composition of test environment for the investigation of various issues related to the processing of satellite accelerations
3	**Gravity field processing** Implementation of functional and stochastic models of accelerations used as pseudo-observations, computation of CHAMP and GOCE gravity field models
4	**Comparison and validation of computed gravity field models** Implementation of software for validation, preparation of a validation report

Due to the splitting of the Institute of Navigation and Satellite Geodesy into two separate parts and to the introduction of a new software package by the new head of the newly founded Institute of Theoretical Geodesy and Satellite Geodesy, Univ.-Prof. Dr.-Ing. Torsten Mayer-Gürr some changes have been made to the proposed work packages. A detailed description of the changes made can be found under chapter 2.4 Revised work package description.

2.3 Contractual matters

Meeting plan

According to the project proposal the following meetings were held:

Meeting	Date & place
Kick-off Meeting	01.04.2011, Graz
Midterm Meeting	30.11.2011, Graz
Final Meeting	19.10.2012, Graz

Kick-off and midterm meeting were held internally at the ITSG without participation of the FFG. The final presentation meeting was held on 19.10.2012 at the end of phase two.
The two phases of the project lasted for 8 months each and comprised a total of 16 months project duration.

Deliveries

A midterm report was provided on 30.11.2012. The present final report is provided to the FFG concurrently with the final meeting on 19.10.2012.

Scientific presentations

The results achieved so far in this project were presented in an oral presentation at the Deutsche Geodätische Woche 2011 in Nürnberg, Germany held from 27.09.-29.09.2011:

- *Zehentner N., Mayrhofer R., Mayer-Gürr T., Gravitationsfeldbestimmung mittels Beschleunigungsansatz – Untersuchungen zur numerischen Differentiation [29]*

and as a poster at the European Geoscience Union General Assembly 2012 in Vienna, Austria, held from 23.04.-27.04.2012:

- Zehentner N., Mayer-Gürr T., Mayrhofer R., Gravity Field Determination using the Acceleration Approach – Considerations on Numerical Differentiation [30]

Univ. Prof. Dr.-Ing. Torsten Mayer Gürr

2.4 Revised work package description

Due to the fact that the Institute of Navigation and Satellite Geodesy has been split into the Institute of Navigation and the Institute of Theoretical Geodesy and Satellite Geodesy, some new developments had to be considered. Therefore some changes had to be made to the proposed work packages as well as some changes in the scientific staff occurred.
In the following tables changed parts of the work packages are printed **bold**.

WP 0	Scientific and administrative management
Inputs	Project proposal
	Project contract
	Kick-off meeting
Tasks	Management, coordination and controlling of activities
	Control of time schedule and project milestones
	Preparation of documents
Output	Midterm report and final summary report

WP 1	Processing of satellite accelerations
Inputs	Standards
	Various existing software modules
Tasks	Algorithm design of numerical differentiators • **Polynomial interpolation** • Newton Gregory interpolation • Taylor-MacLaurin differentiator
	Processing of satellite accelerations from orbit data
	Pre-processing tasks like outlier detection and data gap handling
	Comparison of differentiators
	Algorithm design for covariance propagation of orbit errors
	Numerical stability
Outputs	Software implementation
	Software modules
	Satellite accelerations

In work package 1 the task *3-point differentiator* was deleted from the list of investigated approaches. On the other hand a few things were added. *Polynomial interpolation* was added to the investigated differentiators. Also two new tasks were introduced. In the task *Numerical stability* the focus lies on investigations concerning the susceptibility of the differentiators for computational effects. The second new task *Comparison of differentiators* examines the properties of the different algorithms.

WP 2	Numerical studies
Inputs	Software system (WP 1)
	Simulated orbit products
	Standards
	Various existing software modules
Tasks	Implementation of noise-free scenario
	Implementation of noise scenarios
	Comparison of derived satellite accelerations based on the implemented differentiators
	Quality assessment
Outputs	Test environment
	Definition of baseline differentiator
	Study report

WP 3	Gravity field processing
Inputs	Software system (WP 1)
	Baseline differentiator (WP 2)
	Models (e.g. temporal variations)
	Standards
	Orbit data and accelerometer data
	Various existing software modules
Tasks	Formulation of functional model
	Formulation of stochastic model
	Assembling of pseudo-observation vector from gravitational, non-gravitational, and satellite accelerations
	Assembling of equation system
	Estimation of CHAMP gravity field models
	Estimation of GOCE gravity field models

Outputs	Software modules
	CHAMP gravity field model based on orbit and accelerometer data
	GOCE gravity field model based on orbit and accelerometer data
	Combined GOCE and CHAMP gravity field model based on orbit and accelerometer data
	Full covariance matrix of each model

In work package 3 the point GOCE gravity field model based on orbit, accelerometer and gradiometer data was replaced by the production of a combined GOCE – CHAMP model.

WP 4	Comparison and validation of computed gravity field models
Inputs	Gravity field models (WP 3) Various existing software modules
Tasks	Software implementation/upgrade for validation
	Validation of gravity models in spatial domain, frequency domain and a direct comparison of the model coefficients
Output	Validation report

In work package 4 the task description has been changed to reflect the more comprehensive validation.

Scientific staff

- Torsten Mayer-Gürr, Senior Scientist
  Head of Institute of Theoretical Geodesy and Satellite Geodesy (ITSG)
- Norbert Zehentner, Scientist
- Reinhard Mayrhofer, Scientist
- Florian Heuberger, Scientist
- Christian Pock, Scientist

3 WP 1 - Processing of satellite accelerations

3.1 Inputs

The inputs for this work package are more or less theoretical. Therefore the following chapter 3.1.1 Gravity field determination using orbit information gives a brief description of gravity field determination from orbit information in general and of the acceleration approach and how it works in detail. A short explanation of the software which is used in the whole project is give in section 3.1.2 Used software package.

3.1.1 Gravity field determination using orbit information

Gravity field

Gravity is a fundamental force which causes the attraction between two bodies. This was first described by Newton in his law of universal gravitation. It states that two masses attract each other with a force that is proportional to the product of their masses and inversely proportional to the square of the distance between them. Also the Earth has its own gravity field which is not constant over the whole world. Therefore the gravitational potential V a function of the position on the Earth. As described in Heiskanen and Moritz [13] V can be modeled using a spherical harmonic expansion depending on the spherical coordinates r, θ and λ .

$$V(r,\theta,\lambda)=\frac{GM}{R}\sum_{l=0}^{\infty}\left(\frac{R}{r}\right)^{l+1}\sum_{m=0}^{l}\bar{P}_{lm}(\cos\theta)\left[\bar{C}_{lm}\cos m\lambda+\bar{S}_{lm}\sin m\lambda\right] \tag{3.1}$$

r	...	distance to geocenter
θ	...	geographical co-latitude
λ	...	geographical longitude
G	...	gravitational constant
M	...	earth's mass
R	...	earth's reference radius
$\bar{P}_{lm}$	...	fully normalized Legendre polynomials of degree l and order m
$\bar{C}_{lm},\bar{S}_{lm}$	...	fully normalized spherical harmonic coefficients of degree l and order m

The first derivative of the potential yields an acceleration. This enables a connection between the accelerations acting on the satellite and the underlying gravity field.

$$\ddot{r}=\nabla V=\nabla\left(\frac{GM}{r}\right)=-\frac{GM}{r^2} \tag{3.2}$$

Formula 3.2 would only be valid if the Earth would be a symmetrical sphere with uniform mass distribution. But this is not true so the potential V is replaced by formula 3.1 and the connection between the Earth's gravity field and the satellites motion is established.

So the following gravity field determination based on precise orbit information is explained in more detail. The idea of extracting the gravity field from satellite orbit information is not new. Since the launch of the first artificial satellites, their positions are observed and used to gather information about the Earth's gravity field. However, the use of satellite-to-satellite tracking in high-low (SST-hl) mode and the launch of dedicated gravity field missions like CHAMP, GRACE or GOCE, the amount of measurements and their distribution over the Earth is good enough to generate global gravity field models without gaps and homogeneous accuracy.
In case of SST-hl the position of a Low Earth Orbiter (LEO) is determined using measurements to the GPS satellites positioned in higher orbits. There exist two ways to use the GPS observations for gravity field determination:

- direct use of the pseudo-range and phase range observations
- compute positions out of the GPS measurements and estimation of a gravity field model using them as pseudo observations

The first possibility is also called *the classical method* [25], e.g. used at the Geoforschungszentrum Potsdam (GFZ). In case of the second technique we have to make further distinctions between different approaches. Three of the most important methods are:

- Short arc integral approach
- Energy balance approach
- Acceleration approach

All three methods have been successfully used for gravity field determination. Until now the acceleration approach is the least common one. In this project some aspects of the acceleration approach are investigated in detail, therefore a description is given in the next chapter. The remaining methods will not be further discussed.

Acceleration approach

The acceleration approach has already been used to determine the gravity field of planets or also in flight gravimetry. For observing the Earth's gravity field it was firstly used and investigated by Austen and Reubelt [1] in the frame of a master thesis.
In principle the acceleration approach is based on newton's second law of motion:

$$F = m \cdot \ddot{r} \tag{3.3}$$

In case of a satellite's position in his orbit this means:

$$\ddot{r}(t) = f(t) \tag{3.4}$$

Equation 3.4 is valid only in an inertial reference system. It states that the accelerations $\ddot{r}$ at the time t depend only on the mass specific force $f(t)$ acting on the satellite at this moment This mass specific force $f(t)$ consists of all forces acting on the satellite no matter what origin they have. This encloses gravitational forces of the Earth and other celestial

bodies like the moon, the sun and other planets. Furthermore $f(t)$ includes also forces that are non gravitational. These so called non-conservative forces are caused by solar radiation pressure, earth albedo, atmospheric drag, aerodynamic effects due to the shape of the satellite and eventually the thrusters used to control the satellite's attitude. If we consider formula 3.4 in a non-inertial reference frame, additional apparent accelerations occur. In the inertial frame however the observed accelerations can be directly connected to the gravity potential of the Earth. Only the non-conservative forces and the tidal forces have to be subtracted from the observations. After that, only accelerations caused by Earth's gravity field remain. The non-gravitational forces are observed by an accelerometer on board of the satellite and can be applied directly. The tidal forces caused by moon, sun and other planets can be modeled sufficiently well. Therefore they are computed using the latest model. After correcting all influences, the pure accelerations caused by the Earth's gravity field remain and can be used to determine a spherical harmonic model incorporating formula 3.1 and 3.2.

A major challenge is the acceleration determination. They are not observed directly and therefore must be computed from positions using numerical differentiation. This can be done in different ways. Some of the most popular methods are:

- Polynomial interpolation
- 9-point Newton-Gregory differentiation
- Taylor-MacLaurin differentiation
- ...

All of them carry out the differentiation in the time domain. There is also a possibility to accomplish the differentiation in the frequency domain. Therefore the signal, in this case the positions of the satellite at equidistant time intervals, must be transformed into the frequency domain by means of a Fourier transformation. The differentiation is done by multiplying the produced frequency response by ω^2 where ω represents the circular frequency. Afterwards, the modified signal is transformed back into the time domain which provides the accelerations as the result. The main disadvantage of the approach in frequency domain is the need of constant sampled and data gap-free observations. If data gaps occur the data cannot be differentiated as a whole. [25]

The methods used for differentiation of positions to derive accelerations are described in more detail in chapter 3.2.1 Algorithm design. All differentiation methods have in common that a function is fitted to the positions and subsequently this function is differentiated analytically and evaluated at the desired time with the estimated coefficients. Just the type of function used, the degree of the used function, the number of used data points and whether the function is calculated with or without overdetermination vary. All methods evaluate the function at the central time to minimize the differentiation error. By assuming constant sampling another advantage emerges: the whole calculation becomes a linear combination of the positions around the central time. This means that the differentiation

operator can be used like a moving window function known from image or signal processing. As long as the positions are equally weighted the coefficients of the window function remain constant and therefore have to be computed only once.
The following table shows in which cases the coefficients are constant or not.

	overdetermination	
weighting	yes	no
yes	not constant	constant
no	constant	constant

Table 1: connection between weighting and overdetermination.

3.1.2 Used software package

As already mentioned before the Institute for Theoretical Geodesy and Satellite Geodesy was founded in 2011 out of a part of the former Institute for Navigation and Satellite Geodesy. Torsten Mayer-Gürr became the newly appointed head of institute. Previously he was working at the University of Bonn at the Institute for Geodesy and Geoinformation. In the frame of his doctoral thesis and in cooperation with other scientists the software package GROOPS (Gravity Recovery Object Oriented Programming System) was created [17]. He brought this software to the Institute of Theoretical Geodesy and Satellite Geodesy which was used in this project. The following section gives a short description about the functionality of this software.

GROOPS

GROOPS has been developed and implemented at the Institute for Geodesy and Geoinformation of the University of Bonn since the year 2002. GROOPS is a modular software package for gravity field computations and uses the benefits of object oriented programming. It is almost completely written in C++. This makes the whole package very flexible and provides many opportunities for extensions and modifications without rewriting the whole software. GROOPS can be compiled on machines with different operating systems and it supports parallel computing. So it also runs on a multi computer cluster or it can benefit from running on a PC with a multi-core processor.
The current version of the software provides in general the following capabilities:

- In-/Output of various data formats for various instrument types
- Simulation of various observation types
- Observation handling (reduce, interpolate, filter, partition, ...)
- Gravity field recovery from ...
  - precise kinematic orbits

    - precise inter-satellite observations
    - satellite gravity gradiometry
    - terrestrial data
- global or regional gravity field determination
- gravity field representation by spherical harmonics or spherical splines
- static and temporal gravity field models
- Simulation or real data processing

Subsequently the whole procedure for processing a gravity field is explained exemplary. Therefore only the parts needed for this purpose are mentioned explicitly. These parts also correspond to the ones used in the present project. Programs or classes which are part of GROOPS will be displayed ***bold*** and ***italic***. In general the programs and the associated work flow are the same for real and simulated data.

The only difference is the fact that in a simulation the observation files have to be simulated. This is done with the programs ***SimulateOrbit***, ***SimulateStarCamera***, ***SimulateGradiometer***, ***SimulateAccelerometer*** and more. All these programs produce an output file which contains the simulated data.

In case of real observation data each satellite mission has its own file formats. Therefore, the data must be converted into the GROOPS format. For file conversion there are a lot of programs available. They are grouped together and they are named after the conversion they make. For example ***GraceCSR2Orbit***, ***GoceXml2Orbit*** or ***Igs2GpsOrbit*** are programs to read different orbit files and they all produce an output file in GROOPS format which looks the same in each of the three cases.

After the whole data is prepared the processing chain is the same for simulated and real data. The next step is to split the time series of observations into short arcs. These arcs contain no data gaps and make the processing of the whole gravity field much faster. The splitting is done with the program ***ArcDesigner*** and produces an output file which now contains the observations split into short time series. The length of the arcs is defined by the user. If a data gap occurs in the input file the arc is ended and after the data gap a new arc starts. The user also defines a minimum length for the arcs. If there are arcs between two data gaps which would be shorter than the defined minimum length then the arc is eliminated.

In the case of real data, the different data files of the instruments may have slightly different time stamps. Hence they must be synchronized before processing them. This can be done with the program ***ArcSynchronize***. The next step is to accumulate the normal equations. Therefore the program ***NormalsBuild*** is provided. It sets up the whole system of equations. The most important inputs for this program are as follows:

- Output file name
- Type of estimation approach
    - ***PodIntegral***

    - ***PodEnergy***
    - ***PodAcceleration***
    - ***SatelliteTracking***
    - ***Gradiometer***
    - ***Terrestrial***
    - ***RelativisticClock***
- Right hand side
    - Input file (orbit, accelerometer, ...)
    - Reference field
    - Tide models
    - and different options depending on the used approach
- Input files (orbit, star camera, ...)
- Earth rotation
    - ITRF 2010, ITRF 2003, ITRF 1996, gmst, era, z-axis
- Representation
    - ***Spherical harmonics***
        - minimum degree
        - maximum degree
    - ***Radial bases***
    - ***Time trend***
    - ***Time Fourier***
    - ***Time splines***
    - ***Doodson harmonic***
- and further options which differ between the estimation approaches.

In this program, the core definitions are made. Like the maximum degree of the estimated gravity field or whether the covariances of the orbit positions are used or not. The above mentioned options are not complete and the different representations or estimation approaches all have their own options which control their behavior. But mentioning all of them would be far too much for this report.

The next step is to solve the accumulated normal equations with the program ***NormalsSolverVCE.*** The input for this program are the accumulated normal equations saved in a file or you can directly integrate the functionality of ***NormalsBuild*** into this program. Several output files are available for saving the estimated parameter vector, the standard deviations of the parameter, the full covariance matrix and others.

The next program to execute is ***Gravityfield2PotentialCoefficients.*** This program converts the output of ***NormalsSolverVCE*** to potential coefficients and combines it either with an a priori subtracted reference field or with a negative reference field to find the difference between two fields. The result is then saved in an output file which contains the potential

coefficients. After this step the computed gravity field is finished and can be used for further analysis or visualization.
Afterwards, in most cases a visualization of the results follows. Therefore a few different programs exist. For example ***PlotDegreeVariances***, ***Gravityfield2GriddedData***, ***PlotGriddedData*** or ***PlotSpericalHarmonicsTriangle*** are the four most important.
All in all this sketches the work flow of processing a gravity field model with simulated or real data. Beyond that, GROOPS comprises much more programs for solving other tasks.

PodAcceleration

PodAcceleration is an observation class in GROOPS and is the main part which was written during this project to implement the different approaches for the task of numerical differentiation. **POD** stands for **P**recise **O**rbit **D**ata and is widely used as acronym for tasks which are related to precise kinematic orbits.
In general, this class provides the functionality to produce accelerations from orbit positions by means of numeric differentiation and then set up the normal equations for the estimation process.

GROOPS Interface

GROOPS itself is a command line program and is configured using XML files. Editing this XML files is possible in a simple text editor. But to make it easier to use GROOPS, a graphical user interface is provided for editing the XML files named ***groopsinterface***. GROOPS can be launched directly from within this interface with the desired configurations without editing the XML file by hand.

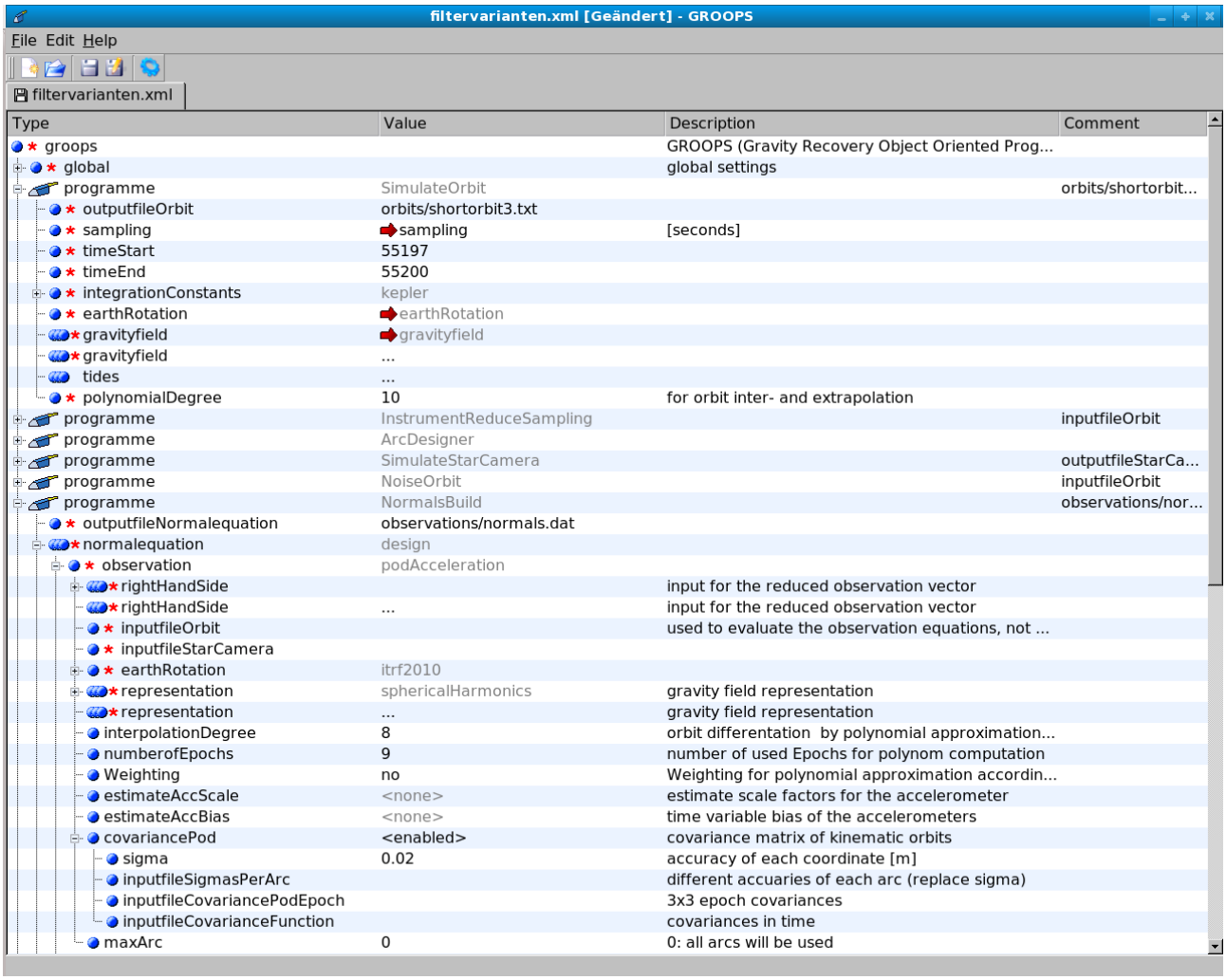

Figure 1: Screen shot of groopsinterface to configure XML files.

Figure 1 shows a screen shot of the graphical user interface for editing the configuration XML files. Any number of programs can be combined one after another. When starting GROOPS from the interface one can then decide which of the listed programs should be run. Lines with a blue dot in front are the options of a specific program. If there is a red star then this option must be set, otherwise the program does not run. If there are three blue dots then this option can be set several times. Some variables can be set globally, which is then indicated by the red arrow in front of the name. This is helpful if one variable is needed by different programs. If you set it global you have to change it only once in case of changing your configuration. Otherwise you would have to change it in every program for yourself.

All in all this interface enables the user to configure GROOPS easily with the mouse. The user doesn't need to know anything about the structure or the content of the XML file which is generated.

3.2 Tasks

3.2.1 Algorithm design

The first task of this work package includes the algorithm design for the different methods of numerical differentiation. In the following three sections the three selected differentiators are explained.

Polynomial interpolation

The first variant of the classical approach towards numerical differentiation is the polynomial interpolation or approximation. Depending on whether the estimation of the polynomial is overdetermined or not it is called approximation or interpolation. A chosen polynomial of a certain degree is adapted to the data points by means of a least squares adjustment and afterwards differentiated analytically. The numerical evaluation of the differentiated polynomial provides the solution at the desired point in time.

Based on the time series of satellite positions $r(t)$, the second order derivative $\frac{r(t)}{dt^2}=\ddot{r}(t)$ has to be obtained. To achieve that, a polynomial of a preliminary chosen degree is set up to accurately approximate the time series. The polynomial is expressed as

$$r(t_0+\tau)\approx\sum_{n=0}^{N} c_n \tau^n \,. \tag{3.5}$$

For the estimation of the polynomial the following system of equations is set up

$$\begin{pmatrix} r(t_0+\tau_0) \\ . \\ . \\ r(t_0+\tau_M) \end{pmatrix} = \begin{pmatrix} 1 & \tau_0 & \tau_0^2 & . & . & \tau_0^N \\ . & . & . & . & . & . \\ . & . & . & . & . & . \\ 1 & \tau_M & \tau_M^2 & . & . & \tau_M^N \end{pmatrix} \begin{pmatrix} c_0 \\ . \\ . \\ c_N \end{pmatrix} \quad \text{with} \quad \tau_i=(i-\frac{M}{2})\Delta t \,. \tag{3.6}$$

t_0 ... time at which the polynomial is evaluated
τ_i ... time difference between t_0 and the actual data point
M ... number of used data points > N+1
N ... degree of the polynomial
c_i ... polynomial coefficients
Δt ... sampling

Formula 3.6 is valid for determined as well as for overdetermined systems with any degree and any number of data points, but the degree of the polynomial should be even and the number of data points odd. This is to guarantee a symmetrical distribution around the central time at which the polynomial is evaluated later.
The estimation of the coefficients is done by a classical least squares adjustment were the square sum of the residuals is minimized. The linear system reads

$$\boldsymbol{l}+\boldsymbol{v}=\boldsymbol{A}\boldsymbol{x}\,. \tag{3.7}$$

It can be solved by means of least squares adjustment, where the square sum of the residuals is minimized by

$$\hat{\boldsymbol{x}}=(\boldsymbol{A}^T\boldsymbol{P}\boldsymbol{A})^{-1}\boldsymbol{A}^T\boldsymbol{P}\boldsymbol{l}\,. \tag{3.8}$$

$\hat{\boldsymbol{x}}$ are the estimated parameters, in this case the coefficients of the chosen polynomial. $\boldsymbol{A}$ is the design matrix built up like stated in formula 3.6. $\boldsymbol{P}$ is the weight matrix for the observations. It can be a unit matrix or it is the inverse of the covariance matrix of the observations. $\boldsymbol{l}$ contains the observations. Here, it is the satellite position at different times. If we now combine the matrix multiplication $(\boldsymbol{A}^T\boldsymbol{P}\boldsymbol{A})^{-1}\boldsymbol{A}^T\boldsymbol{P}$ to the new matrix $\boldsymbol{W}$ then the lines of $\boldsymbol{W}$ are linear combinations of the observations to obtain the coefficients of the polynomial.

But rather sought is the second derivative of the polynomial than the polynomial itself. So we can take formula 3.5 and differentiate it twice which then provides the following formula

$$\ddot{r}(t_0+\tau)=\sum_{n=2}^{N} c_n(n-1)n\tau^{(n-2)}\,. \tag{3.9}$$

Under the assumption that the time series has a constant sampling and as mentioned before that the polynomial is evaluated at the central point, τ becomes 0 and so the expression $c_n(n-1)n\tau^{(n-2)}$ remains only for $n=2$. This leads to the relation

$$\ddot{r}(t_0)=2c_2\,. \tag{3.10}$$

Thus only the coefficient c_2 is necessary for getting the second derivative of the polynomial. This is as stated above a linear combination of the incorporated observations. The coefficients of this linear combination are in the third row of the matrix W. As already listed in Table 1 in most cases these coefficients are constant. They now make up the kernel of the moving window function which will be applied as filter kernel as displayed in Figure 2.

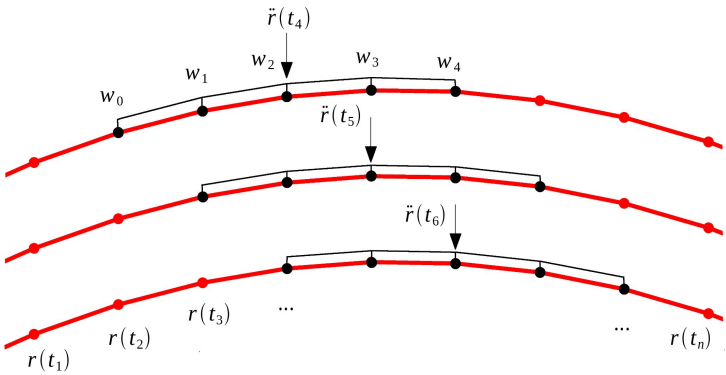

Figure 2: application scheme of a moving window function.

As an example the coefficients of a polynomial with degree 6 and without overdetermination are listed below. Assumed sampling of the time series is 5 seconds.

w_0	w_1	w_2	w_3	w_4	w_5	w_6
0.00044	-0.00600	0.06000	-0.10889	0.06000	-0.00600	0.00044

Partially the same observations are used for the computation of temporally neighboring accelerations. Therefore, the produced accelerations are correlated to each other, no matter if the used positions are already correlated.

The application of the moving window function can be combined to a matrix, which contains the filter coefficients in each line, each shifted by one column

$$\boldsymbol{F}=\begin{pmatrix} w_0 & w_1 & w_2 & \dots & w_M & 0 & 0 & \cdot \\ 0 & w_0 & w_1 & w_2 & \dots & w_M & 0 & \cdot \\ 0 & 0 & w_0 & w_1 & w_2 & \dots & w_M & \cdot \\ \cdot & \cdot & \cdot & \cdot & \cdot & \cdot & \cdot & \cdot \end{pmatrix}. \tag{3.11}$$

The required accelerations are now found by the following multiplication

$$\ddot{\boldsymbol{r}}=\boldsymbol{F}\,\boldsymbol{r}\,. \tag{3.12}$$

According to the law of variance propagation the covariance matrix of the accelerations is given by

$$\boldsymbol{\Sigma}_{\ddot{r}\ddot{r}}=\sigma^2\,\boldsymbol{F}\,\boldsymbol{\Sigma}_{rr}\,\boldsymbol{F}^T\,. \tag{3.13}$$

Newton Gregory interpolation

The interpolation according to the scheme of Newton-Gregory is based on a polynomial of a certain degree n. The calculation is done by using the Newtonian polynomials and the so called forward differences.

Starting point is the following formula [25]

$$\begin{aligned} R(t)&=r(t_1+q\,\Delta t)=r(t_1)+\binom{q}{1}\Delta^{1}_{3/2}+\binom{q}{2}\Delta^{2}_{2}+\dots+\binom{q}{n-1}\Delta^{n-1}_{1+(n-1)/2}= \\ &=r(t_1)+\sum_{i=1}^{n-1}\binom{q}{i}\Delta^{i}_{1+i/2}; \qquad q\in[0,n-1] \end{aligned}\,. \tag{3.14}$$

Therefore the forward differences are defined as

$$\Delta^{i}_{1+i/2}=\sum_{j=1}^{i+1}(-1)^{i+j+1}\binom{i}{j-1}r(t_j)\,. \tag{3.15}$$

$R(t)$	...	interpolation function
$r(t_i)$	...	position at the time t_i
$r(t_1+q\Delta t)$	...	position at the evaluation time
t_1	...	starting time of interpolation
t_n	...	end time of interpolation
n	...	number of contributing positions
Δt	...	sampling
$q=(t-t_1)/\Delta t$	...	quotient of time difference

To get the accelerations the interpolation function $R(t)$ is differentiated by the time twice. This means that the Newtonian polynomials must also be differentiated by the time because they contain the starting time and the time of the current data point. According to Reubelt [25] this leads to the following formula

$$\ddot{R}(t)=\binom{q}{1}'' \Delta^{1}_{3/2}+\binom{q}{2}'' \Delta^{2}_{2}+\ldots+\binom{q}{n-1}\Delta^{n-1}_{1+(n-1)/2}=\sum_{i=1}^{n-1}\binom{q}{i}'' \Delta^{i}_{1+i/2}\,. \tag{3.16}$$

With the second derivatives of the Newtonian polynomials

$$\begin{aligned}
\binom{q}{1}'' &= 0 \\
\binom{q}{2}'' &= \frac{1}{\Delta t^2} \\
\binom{q}{3}'' &= \frac{1}{\Delta t^2}(q-1) \\
\binom{q}{4}'' &= \frac{1}{\Delta t^2}\frac{12q^2-36q+22}{24} \\
\binom{q}{5}'' &= \frac{1}{\Delta t^2}\frac{20q^3-120q^2+210q-100}{120}
\end{aligned} \tag{3.17}$$

Evaluating all expressions yields again a linear combination of the observations to get the accelerations. This again can be interpreted as a moving window function which must be applied to the time series of positions. In this case there is no possibility to introduce an overdetermination. Due to this fact the filter kernel remains constant in under every circumstances. The numerical values of this filter are solely dependent on the used sampling. For example the coefficients of a 7-point scheme are according to Reubelt [25]

w_0	w_1	w_2	w_3	w_4	w_5	w_6
$\frac{1}{90\Delta t^2}$	$\frac{-3}{20\Delta t^2}$	$\frac{3}{2\Delta t^2}$	$\frac{-49}{18\Delta t^2}$	$\frac{3}{2\Delta t^2}$	$\frac{-3}{20\Delta t^2}$	$\frac{1}{90\Delta t^2}$

(3.18)

Assuming now a sampling of 5 seconds this yields the following numeric values

w_0	w_1	w_2	w_3	w_4	w_5	w_6
0.00044	-0.00600	0.06000	-0.10889	0.06000	-0.00600	0.00044

Compared to the example given in the section of polynomial interpolation it is noticeable that the values are exactly the same. This is true when comparing polynomial interpolation without overdetermination against Newton-Gregory interpolation with the same amount of contributing data points. It is numerically shown that Newton-Gregory interpolation and polynomial interpolation provide the same results. Therefore it is irrelevant which of the two methods is used to compute the filter coefficients.

Taylor-MacLaurin differentiator

The first derivative

The Taylor-MacLaurin differentiation was already used by Badura [2] [3] and Jandrisevits [14]. They used it to derive velocities for the energy balance approach. A detailed investigation was made by Goiginger [9]. In this project, the algorithm shall for the first time be used to derive the second derivative, the accelerations. In general the Taylor-MacLaurin differentiation is based on a Taylor series expansion in every data point. Furthermore the data points are combined to differences which are then used to derive the derivatives. These differences are defined as follows

$$\Delta_k^{\,j} = \frac{r_{k+j} - r_{k-j}}{2\,j\,\Delta t}\,.$$

r_k	...	value of the function at the central point k
r_{k+j}	...	value of the function at the point k+j
r_{k-j}	...	value of the function at the point k-j
j	...	width of the differencing
Δt	...	constant sampling

(3.19)

Now a Taylor series expansion in the two used data points r_{k+j} and r_{k-j} is assumed

$$r_{k+j} = r_k + j\,dt\,r_k' + \frac{1}{2}j^2 dt^2 r_k'' + \frac{1}{6}j^3 dt^3 r_k''' + \frac{1}{24}j^4 dt^4 r_k^{IV} + \frac{1}{120}j^5 dt^5 r_k^{V} + \frac{1}{720}j^6 dt^6 r_k^{VI} + \ldots \tag{3.20}$$

$$r_{k-j} = r_k - j\,dt\,r_k' + \frac{1}{2}j^2 dt^2 r_k'' - \frac{1}{6}j^3 dt^3 r_k''' + \frac{1}{24}j^4 dt^4 r_k^{IV} - \frac{1}{120}j^5 dt^5 r_k^{V} + \frac{1}{720}j^6 dt^6 r_k^{VI} - \ldots\,. \tag{3.21}$$

If we now insert formula 3.20 and 3.21 into equation 3.19 the following formula is obtained

$$\Delta_k^{\,j} = r_k' + \frac{1}{6}j^2 dt^2 r_k''' + \frac{1}{120}j^4 dt^4 r_k^{V} + \ldots\,. \tag{3.22}$$

Now these relations can be written as $\boldsymbol{l} = \boldsymbol{A}\,\boldsymbol{x}$ which is the classical starting point for a least squares adjustment. The elements of the design matrix are obtained by the following equation

$$A(j-1,(n-1)/2)=\frac{\Delta t^{n-1}\, j^{n-1}}{n!}.$$

j = 1, 2, ... (m-1)/2
n = 1,3,5,7, ... highest derivative
m ... number of contributing observations (3.23)

$$\boldsymbol{l}=\begin{bmatrix}\Delta_k^{\,1}\\ \Delta_k^{\,2}\\ \Delta_k^{\,3}\\ \cdot\end{bmatrix}\quad \boldsymbol{A}=\begin{bmatrix}1 & \frac{1}{6} & \frac{1}{120} & \cdot\\ 1 & \frac{4}{6} & \frac{16}{120} & \cdot\\ 1 & \frac{9}{6} & \frac{81}{120} & \cdot\\ \cdot & \cdot & \cdot & \cdot\end{bmatrix}\quad \boldsymbol{x}=\begin{bmatrix}r_k'\\ dt^2 r_k'''\\ dt^4 r_k^V\\ \cdot\end{bmatrix} \tag{3.24}$$

The solution for this system of equations is gained by the classical least squares procedure in dependency whether a weight matrix is used or not

$$\hat{\boldsymbol{x}}=(\boldsymbol{A}^T\boldsymbol{A})^{-1}\boldsymbol{A}^T\boldsymbol{l} \quad \text{or} \quad \hat{\boldsymbol{x}}=(\boldsymbol{A}^T\boldsymbol{P}\boldsymbol{A})^{-1}\boldsymbol{A}^T\boldsymbol{P}\boldsymbol{l}. \tag{3.25}$$

Furthermore the formulation of the differences Δ_k^j can be combined into one matrix. Then the differences are built up with the following equation

$$\boldsymbol{l}=\boldsymbol{F}\,\boldsymbol{l}_{orig.}. \tag{3.26}$$

Here $\boldsymbol{l}_{orig.}$ contains the original satellite positions and the Matrix $\boldsymbol{F}$ has the form

$$\boldsymbol{F}=\begin{bmatrix}\cdot & 0 & 0 & \frac{-1}{2j\Delta t} & 0 & \frac{1}{2j\Delta t} & 0 & 0 & \cdot\\ \cdot & 0 & \frac{-1}{2j\Delta t} & 0 & 0 & 0 & \frac{1}{2j\Delta t} & 0 & \cdot\\ \cdot & \frac{-1}{2j\Delta t} & 0 & 0 & 0 & 0 & 0 & \frac{1}{2j\Delta t} & \cdot\\ \cdot & \cdot & \cdot & \cdot & \cdot & \cdot & \cdot & \cdot & \cdot\end{bmatrix}. \tag{3.27}$$

The adjustment produces the 1st, 3rd, 5th, ... derivative of the time series at the central point. The matrices $\boldsymbol{A}$ and $\boldsymbol{F}$ are constant as long as the number of differences and the number of estimated derivatives remains the same. Therefore the whole matrix multiplication $(\boldsymbol{A}^T\boldsymbol{P}\boldsymbol{A})^{-1}\boldsymbol{A}^T\boldsymbol{P}\boldsymbol{F}$ is constant as long as the weight matrix $\boldsymbol{P}$ remains constant. According to the variance propagation law $\boldsymbol{P}$ is based on the covariance matrix of the satellite positions.

$$\boldsymbol{P}=\boldsymbol{F}\,\boldsymbol{\Sigma}_{\boldsymbol{l}_{orig}\boldsymbol{l}_{orig}}\boldsymbol{F}^T. \tag{3.28}$$

If the satellite positions are assumed to have the same standard deviation at every epoch, then the whole multiplication remains constant for every epoch. Otherwise if the variance and covariance information of the satellite positions is used, this computation has to be done separately for every epoch. No matter if the matrices are constant or not the first line

of $(\boldsymbol{A}^T \boldsymbol{P}\, \boldsymbol{A})^{-1} \boldsymbol{A}^T \boldsymbol{P}\, \boldsymbol{F}$ contains the coefficients of the linear combination of orbit positions to obtain the first derivative. In case of constant matrices this line can again be interpreted as moving window function and applied to the whole time series of satellite positions.

The second derivative

In the previous section, the Taylor-MacLaurin algorithm for calculating the first derivative was explained. This implementation only provides the first, the third and the fifth derivative and so on depending on how many are estimated. But for the acceleration approach the second derivative is needed. Therefore the implementation used so far must be extended. To do so there are two possibilities:

- After computing the first derivative of the positions which corresponds to the velocities the same algorithm is again applied on the outcome. This yields the first derivative of the first derivative which is the second derivative of the original time series. This means that in case of a constant filter function this filter is applied twice. Therefore the two filter functions can also be combined beforehand by means of convoluting them. This generates a new filter which directly provides the second derivative. If the number of parameters and contributing data points remains the same, it is a convolution of the filter with itself.

- The second possibility is to extend the definition of the Taylor-MacLaurin algorithm in a way that it provides directly the second derivative. This extension is described in the following section.

In this project the second opportunity is chosen, because the first one would mean that two different polynomials are fitted to the time series. The first one to the time series of the satellite positions and the second one to the derived time series of satellite velocities. The second possibility on the other hand provides directly the accelerations. Also the computational burden for the second approach is less than for the first one and additionally the variance propagation is simpler.

Extended Taylor-MacLaurin algorithm

First step is to extend the definition of the differences described in formula 3.19 to

$$\Delta\Delta_k{}^j = \frac{\Delta^j_{k+j+j} - \Delta^j_{k-j-j}}{2\, j \Delta\, t} \,. \tag{3.29}$$

If now the original definition of the differences Δ^j_{k+j+j} is inserted it leads to

$$\Delta\Delta^j_k = \frac{r_{k+2\mathrm{j}} - 2\, r_k + r_{k-2\mathrm{j}}}{4\, j^2 dt^2} \,. \tag{3.30}$$

And if additionally j is replaced by $j/2$ the following definition of double differences is achieved

$$\Delta\Delta_k^{\frac{j}{2}} = \frac{r_{k+j} - 2r_k + r_{k-j}}{2j^2 dt^2} . \tag{3.31}$$

The contained data points r are again replaced by a Taylor series expansion. This then leads to the expression

$$2\Delta\Delta_k^{\frac{j}{2}} = r_k'' + \frac{1}{12} j^2 dt^2 r_k^{IV} + \frac{1}{360} j^4 dt^4 r_k^{VI} + \dots . \tag{3.32}$$

The formula above can now be used for a least squares adjustment which then provides derivatives 2, 4, 6 and so on for the central time k.

Assuming the same scenario as for polynomial interpolation and Newton-Gregory interpolation, the extended Taylor-MacLaurin algorithm leads to the following numeric values for the filter function.

w_0	w_1	w_2	w_3	w_4	w_5	w_6
0.00044	-0.00600	0.06000	-0.10889	0.06000	-0.00600	0.00044

In this case the adjustment is performed with 3 parameters, the second, the fourth and the sixth derivative and with 7 contributing data points. Thus it is empirically shown that this approach leads to the same filter function like described in sections Polynomial interpolation and Newton Gregory interpolation.

3.2.2 Processing of satellite accelerations from orbit data

This task is ongoing throughout the whole project, because every investigation of certain aspects or every computation of a gravity field model requires the derivation of accelerations from the orbit data. The mathematical model behind the processing of accelerations is described in chapter 3.2.1 Algorithm design. There is no difference whether the used orbit data is simulated or real data. For sake of simplicity no further explanations are given at this point. The used accelerations and how they were derived are explained in the tasks where they were used.

3.2.3 Pre-processing tasks like outlier detection or data gap handling

The implemented software divides the orbit into short arcs before setting up the system of equations. This brings some benefits compared to using the whole continuous data set. First of all a data gap handling is not really necessary, because if a data gap occurs in the orbit data the actual arc is ended and after the gap a new one is started. A little draw back of this approach is that when the amount of data points between two gaps is too short this information is lost. But in general this loss is quite small compared to the overall amount of

data. The second benefit concerns the outlier detection. The implemented software uses the covariance information of the orbit positions to find an appropriate weighting for the single observations. If the covariance information is correct outliers or observations with bad accuracy get little weight and therefore nearly make no contribution to the result. In an iterative process with a variance component estimation the best suitable weight for every arc is determined. If one arc contains an outlier which is not seen in the covariance information the whole arc gets a smaller weight and then the bad observation makes no contribution to the solution any more. Drawback of this approach is the fact that also the good observations of this arc get a smaller weight and so some information is lost. But again the loss of information can be neglected due to the huge amount of available data. Due to these two facts no explicit pre-processing tasks have to be performed. Handling data gaps and outliers is some kind of integrated into the whole gravity field estimation process.

3.2.4 Comparison of differentiators

Based on the algorithm design described in chapter 3.2.1 and on numerical evaluations, a comparison of the three involved approaches can be done. Based on so far mentioned numeric examples an assumption can be made: all approaches deliver the same results!

Newton-Gregory interpolation vs. polynomial interpolation

The Newton-Gregory interpolation is as mentioned before based on the Newtonian base polynomials and on the forward differences. There is no possibility to introduce an overdetermination and the final result depends only on the used sampling interval. According to Reubelt [25] who evaluates the interpolation for the 3-, 5-, 7- and 9-point scheme this then provides the following filter coefficients

$$\begin{array}{ccccccccc}
 & & & \frac{1}{\Delta t^2} & \frac{-2}{\Delta t^2} & \frac{1}{\Delta t^2} & & & \\
 & & -\frac{1}{12\Delta t^2} & \frac{4}{3\Delta t^2} & -\frac{5}{2\Delta t^2} & \frac{4}{3\Delta t^2} & -\frac{1}{12\Delta t^2} & & \\
 & \frac{1}{90\Delta t^2} & \frac{-3}{20\Delta t^2} & \frac{3}{2\Delta t^2} & \frac{-49}{18\Delta t^2} & \frac{3}{2\Delta t^2} & \frac{-3}{20\Delta t^2} & \frac{1}{90\Delta t^2} & \\
-\frac{1}{560\Delta t^2} & \frac{8}{315\Delta t^2} & -\frac{1}{5\Delta t^2} & \frac{8}{5\Delta t^2} & -\frac{205}{72\Delta t^2} & \frac{8}{5\Delta t^2} & -\frac{1}{5\Delta t^2} & \frac{8}{315\Delta t^2} & -\frac{1}{560\Delta t^2}
\end{array} \tag{3.33}$$

If we now assume a constant sampling of 1 second the filters become

			1.0000	-2.0000	1.0000			
		-0.0833	1.3333	-2.5000	1.3333	-0.0833		
	0.0111	-0.1500	1.5000	-2.7222	1.5000	-0.1500	0.0111	
-0.0018	0.0254	-0.2000	1.6000	-2.8472	1.6000	-0.2000	0.0254	-0.0018

Table 2: numeric values for Newton-Gregory 3-, 5-, 7- and 9-point scheme.

In contrast to the Newton-Gregory interpolation the polynomial interpolation gives the opportunity to introduce an overdetermination. But for this comparison we only look at polynomials without overdetermination. And when evaluating polynomials with degree 2, 4, 6 and 8 it provides exactly the same coefficients as shown above in table 2.
So the Newton-Gregory approach has no advantages over the polynomial interpolation. In contrast, the polynomial interpolation is far more flexible because many different constellations of overdetermination and polynomial degrees can be used easily.

Taylor-MacLaurin differentiation vs. polynomial interpolation

Looking at a Taylor series expansion up to the order n shows that in fact it is a polynomial with the degree n

$$r_{k+j} = r_k + j\,dt\,r'_k + \frac{1}{2} j^2 dt^2 r''_k + \frac{1}{6} j^3 dt^3 r'''_k + \frac{1}{24} j^4 dt^4 r^{IV}_k + \frac{1}{120} j^5 dt^5 r^{V}_k + \dots . \tag{3.34}$$

The derivatives of r correspond to the coefficients of a polynomial. If we now set up a least squares adjustment for estimating the derivatives or respectively the coefficients and combine it with the matrix F described in formula 3.27 this leads to a modified design matrix. After removing zero columns, this modified design matrix is equal to the one used for estimating the Taylor-MacLaurin differentiator.
In the subsequent descriptions the c++ indexing is used which starts at 0 for line or column number 1.
The elements of the design matrix for estimating the polynomial are defined as follows

$$A\left(\frac{m-1}{2}+j, n\right) = \frac{j^n \Delta t^n}{n!} \quad \left(j = -\frac{m-1}{2} \dots 0 \dots \frac{m-1}{2}\right) \text{ and } (n = 0,1,2,\dots degree) . \tag{3.35}$$

m ... number of contributing observations
j ... distance to central time in epochs
n ... degree of polynomial
Δt ... sampling intervall

Now the classic model $\boldsymbol{l} = \boldsymbol{A}\,\boldsymbol{x}$ is extended be the matrix $\boldsymbol{F}$. The matrix $\boldsymbol{F}$ is shown in formula 3.27. This leads to

$$\boldsymbol{F}\,\boldsymbol{l} = \boldsymbol{F}\,\boldsymbol{A}\,\boldsymbol{x} . \tag{3.36}$$

The multiplication of $\boldsymbol{F}$ and $\boldsymbol{A}$ gives the modified design matrix $\boldsymbol{B}$. Their elements are defined as

$$B(j,n) = -\frac{1}{2(-j)\Delta t}\frac{(-j)^n \Delta t^n}{n!} + \frac{1}{2j\Delta t}\frac{j^n \Delta t^n}{n!}. \quad \left(j = 0,1,...\frac{m-1}{2}\right) \text{ and } (n = 0,1,...degree) \tag{3.37}$$

This expression can be simplified dramatically. In the case of an even n it evaluates to 0. If n is odd the formula reduces to

$$B(j,n) = \frac{\Delta t^{n-1} j^{n-1}}{2n!} \quad \left(j = 0,1,...\frac{m-1}{2}\right) \text{ and } (n = 1,3,5,7,...degree). \tag{3.38}$$

Formula 3.38 now is exactly the same as formula 3.23. After removing the zero columns of the matrix B we get the same design matrix as in the case of the Taylor-MacLaurin approach. This shows that both estimations provide the same differentiation method. Here it is proven for the first derivative, because it is easier to show and understand but the same holds for the second derivative.
All in all the Taylor-MacLaurin has no advantages over the classical polynomial interpolation. The polynomial interpolation is more flexible and the introduction of a weight matrix for the observations is easier because in the case of the Taylor-MacLaurin approach a variance propagation must be performed in advance.

Summary

The most important insights gained by the above described investigations and the comparisons between the different methods are:

- Taylor-MacLaurin differentiation, Newton-Gregory interpolation and polynomial interpolation all provide the same results.
- All in all the two special methods can be replaced by the polynomial interpolation.
- The second derivative respectively the accelerations are always a linear combination of the contributing satellite positions.
- There are two methods of getting the second derivative:
  - Computing directly the second derivative of the polynomial.
  - Differentiate the polynomial once and then fitting a new polynomial and differentiate again.
- The two methods provide different results but no advantage could be found.
- Correlations introduced by the filter must be considered.
- These correlations depend on the length of the used filter.
- Previously existing correlations in time between the satellite positions must be taken into account.

Considering all discussed methods and due to the fact that all methods can be replaced by the polynomial interpolation, there is no need to use such special algorithms. They provide no advantages. Moreover the polynomial interpolation has the advantage to be more flexible because overdetermination can be introduced. Furthermore after solving the polynomial by means of a least squares adjustment every possible derivative is at hand without any changes in the design matrix. It must be kept in mind that all the mentioned properties are valid as long as the underlying time series of satellite positions has a constant sampling and the accelerations are evaluated at the central time of the fitted polynomial.
Due to the mentioned facts, only the polynomial interpolation will be used in the following investigations. It provides great flexibility and includes all possible configurations of the other two methods.

3.2.5 Algorithm design for covariance propagation of orbit errors

The implementation of the chosen interpolation method includes also the covariance propagation of orbit errors to errors in the derived accelerations to consequently forward them to the gravity field determination process. This is necessary to get the most accurate estimation for the variances of the derived model.
In case of strictly propagating all covariances of the satellite positions and weighting of observations according to them the whole adjustment process for fitting the polynomial would look like this

$$\hat{\mathbf{x}} = (\boldsymbol{A}^T \boldsymbol{P}\, \boldsymbol{A})^{-1} \boldsymbol{A}^T \boldsymbol{P}\, \boldsymbol{l}\,. \qquad (3.39)$$

$$\boldsymbol{P} = \boldsymbol{\Sigma}_{xx} \qquad \boldsymbol{\Sigma}_{xx} = \textit{covariance matrix of positions for one coordinate direction}$$

As previously outlined the acceleration is then a linear combination of the contributing observations. This can be interpreted as moving window function and the application of this function can be combined to a matrix

$$\boldsymbol{F} = \begin{pmatrix} w_0 & w_1 & w_2 & \dots & w_M & 0 & 0 & \cdot \\ 0 & w_0 & w_1 & w_2 & \dots & w_M & 0 & \cdot \\ 0 & 0 & w_0 & w_1 & w_2 & \dots & w_M & \cdot \\ \cdot & \cdot & \cdot & \cdot & \cdot & \cdot & \cdot & \cdot \end{pmatrix}. \qquad (3.40)$$

Multiplying the positions with the matrix $\boldsymbol{F}$ yields the accelerations

$$\ddot{\boldsymbol{r}} = \boldsymbol{F}\, \boldsymbol{r}\,. \qquad (3.41)$$

According to the law of variance propagation the covariance matrix of the accelerations is now given by

$$\boldsymbol{\Sigma}_{\ddot{r}\ddot{r}} = \sigma^2\, \boldsymbol{F}\, \boldsymbol{\Sigma}_{rr} \boldsymbol{F}^T\,. \qquad (3.42)$$

Depending on the relations stated in Table 1 the lines of F contain always the same filter or not. The derived covariance matrix of the accelerations is then used as input to the gravity

field determination and the observations can be weighted according to their standard deviation.

3.2.6 Numerical stability

As described in the previous chapters the derivation of the accelerations is done by fitting a polynomial to the positions and then differentiate it twice. Therefore the degree of the used polynomial and the number of contributing observations can be chosen freely. Only the following criteria should be considered:

- Degree of the polynomial should be even
- Number of contributing observations should be odd
- Degree < number of observations

The number of observations has to be odd because the polynomial is set up symmetrically around the central time. The degree of the polynomial can be even or odd but both produce the same result for the second derivative. The degree has to be smaller than the number of observations because otherwise the adjustment of the polynomial would fail.
As mentioned in chapter 3.2.1 Algorithm design the polynomial is evaluated at the central time and under the condition that the time series has a constant sampling. Therefore the second derivative becomes a linear combination of the contributing observations and is represented by twice the second coefficient of the polynomial. The design matrix is constant and if no weighting and overdetermination is introduced the resulting linear combination is constant for every epoch and can be applied like a moving window function in signal analysis.
No matter if the filter is constant and computed beforehand or if it is computed for every epoch separately the process is done by a least squares adjustment to find the optimal fitting polynomial. But with increasing degree of the polynomial the adjustment very soon becomes numerically unstable. This is due to the fact that in case of the polynomial fitting the elements of the design matrix have quite big numeric differences and the higher the degree the higher the differences. For this reason some investigations were made concerning different implementations of the adjustment to find the most stable one.
All implementations are based on LAPACK*(Linear Algebra Package)* routines. *LAPACK [37]* is a freely available collection of routines for solving different tasks of linear algebra. These routines are written in Fortran and are optimized concerning their numeric stability.

All in all four implementations were tested:

a) LU decomposition of the design matrix using routine *dgesv*
b) LU decomposition of the normal equation matrix using routines *dgetrf* and *dgetri*
c) LU decomposition of the normal equation matrix using routine *dgesv*
d) QR decomposition of the design matrix using routines *dgegrf, dtrtri* and *dorgqr*

LU decomposition using routine dgesv

The function *solveInPlace* is already part of GROOPS. It is a function to solve a system of equations with no overdetermination and is therefore only applicable in presence of quadratic design matrices. The function inverts the design matrix and multiplies it with the observations vector. SolveInPlace calls the LAPACK routine *dgesv [36].* For solving the system of equations the function *dgesv* uses the LU decomposition.

The following explanation is taken from the code of the routine *dgesv* itself.

```
*  DGESV computes the solution to a real system of linear equations
*     A * X = B,
*  where A is an N-by-N matrix and X and B are N-by-NRHS matrices.
*  The LU decomposition with partial pivoting and row interchanges is
*  used to factor A as
*     A = P * L * U,
*  where P is a permutation matrix, L is unit lower triangular, and U is
*  upper triangular.  The factored form of A is then used to solve the
*  system of equations A * X = B.[36]
```

LU decomposition of N using routine dgetrf and dgetri

This is the classical approach towards solving an overdetermined system of equations by means of the least squares adjustment. The problem therein lies in the inversion of the normal equation matrix. Are the elements of the design matrix numerically very different then the solution of the inversion gets extremely unstable. The current implementation uses the LAPACK functions dgetrf and dgetri for computing the inverse.

The subsequent stated descriptions are taken from the code of the two routines:

```
*  DGETRF computes an LU factorization of a general M-by-N matrix A
*  using partial pivoting with row interchanges.
*  The factorization has the form
*     A = P * L * U
*  where P is a permutation matrix, L is lower triangular with unit
*  diagonal elements (lower trapezoidal if m > n), and U is upper
*  triangular (upper trapezoidal if m < n). [35]

*  DGETRI computes the inverse of a matrix using the LU factorization
*  computed by DGETRF.
*  This method inverts U and then computes inv(A) by solving the system
*  inv(A)*L = inv(U) for inv(A). [34]
```

LU decomposition of N using routine dgesv

This implementation uses again the function *solveInPlace* which in turn uses the LAPACK function *dgesv* to solve the system of equations. Inputs are the normal equation matrix $N=(A^T A)$ and the design matrix A^T as right hand side.

QR decomposition of A using routines dgeqrf, dtrtri and dorgqr

The fourth approach uses the advantages of the QR decomposition to solve the system of equations. Therefore the design matrix $\boldsymbol{A}$ is decomposed into a matrix $\boldsymbol{Q}$ and $\boldsymbol{R}$ such that $\boldsymbol{A}=\boldsymbol{Q}\boldsymbol{R}$. These matrices now have the following properties:

- $\boldsymbol{Q}$ is orthogonal: $\boldsymbol{Q}\boldsymbol{Q}^T=\boldsymbol{I}$
- $\boldsymbol{Q}$ is unitary: $\boldsymbol{Q}\boldsymbol{Q}^{-1}=\boldsymbol{I}$
- $\boldsymbol{R}$ is an upper triangular matrix

The solution of the system is now achieved by $\hat{\boldsymbol{x}}=\boldsymbol{R}^{-1}\boldsymbol{Q}^T\boldsymbol{l}$
For $\boldsymbol{R}^{-1}$ only the upper triangular part with dimension n (number of paramters) is used and inverted. From the matrix $\boldsymbol{Q}$ only the first n columns are used.
In the implementation the *LAPACK* routines *dgegrf*, *dtrtri* and *dorgqr* are used. The short descriptions are taken from the code of the three functions.

```
*  DGEQRF computes a QR factorization of a real M-by-N matrix A:
*  A = Q * R. [33]

*  DTRTRI computes the inverse of a real upper or lower triangular
*  matrix A. [32]

*  DORGQR generates an M-by-N real matrix Q with orthonormal columns,
*  which is defined as the first N columns of a product of K elementary
*  reflectors of order M
*        Q  =  H(1) H(2) . . . H(k)
*  as returned by DGEQRF. [31]
```

Comparison of the four implementations

All four realized implementations provide the result of $\left(\boldsymbol{A}^T\boldsymbol{P}\,\boldsymbol{A}\right)^{-1}\boldsymbol{A}^T\boldsymbol{P}$. This matrix contains the linear combinations to generate all coefficients of the polynomial. As mentioned earlier only the coefficient a_2 is of interest because $2\mathrm{a}_2$ represents the accelerations. This means the third line of the matrix is the desired filter.
Some closed-loop simulations have been carried out with different polynomial degrees to investigate the numeric stability of the four realizations. For sake of simplicity only polynomials without overdetermination are used. Closed-loop means that with the help of a

known gravity field a satellite orbit is simulated. Afterwards, this simulated positions are taken as input for a gravity field determination. Then the estimated gravity field is compared to the used reference field. No noise was added to the positions because then the difference in the results only comes from the implementation of the filter. If the right constellation is chosen then the differences between reference field and estimated gravity field should be as small as possible. The comparison is based on the differences in the degree variances. The degree variances are computed as the rms (root mean square) of all coefficients of the same degree. These variances are then transformed to geoid heights to make the results more illustrative. A detailed description of degree variances is given in section 6.2.1 Comparison of gravity field solutions based on variances. For the comparisons the following satellite constellation was used:

Parameter	Value
Semi-major axis of the orbit	6628000 m
Eccentricity	0,003
Inclination	89,5°
Reference gravity field	GOCO02S [11]
Degree minimum	0
Degree maximum	40
Starting time	01.01.2010 00:00:00
End time	15.01.2010 23:59:59
Sampling	10 seconds
Arc length	120 epochs
Degree minimum for the estimated gravity field	2
Degree minimum for the estimated gravity field	40

Table 3: Satellite constellation for the numerical investigation of different implementations.

Figure 3 shows the results obtained by the four different methods for a polynomial of degree 4 without overdetermination. The black curve is the reference field GOCO02S and the four colored lines display the differences of the four solutions with respect to the reference field. The dashed lines show the estimated variances of the results. All in all the four implementations provide nearly the same results only a few small differences in the low degrees occur.

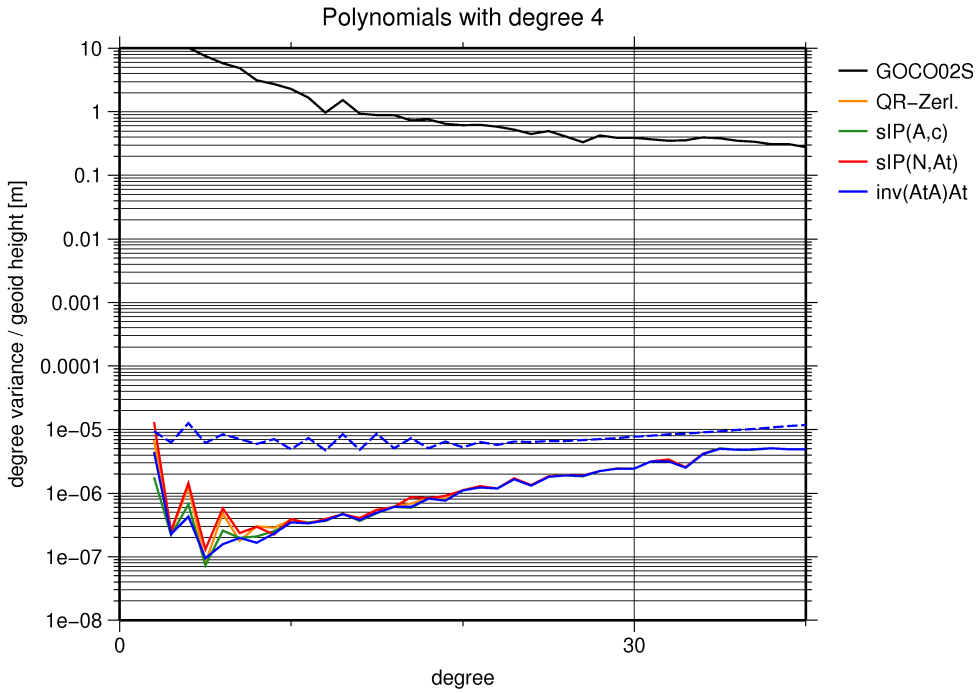

Figure 3: Degree variances with polynomial degree 4. black: reference model GOCO02S, green: implementation a, blue: implementation b, red: implementation c, orange: implementation d.

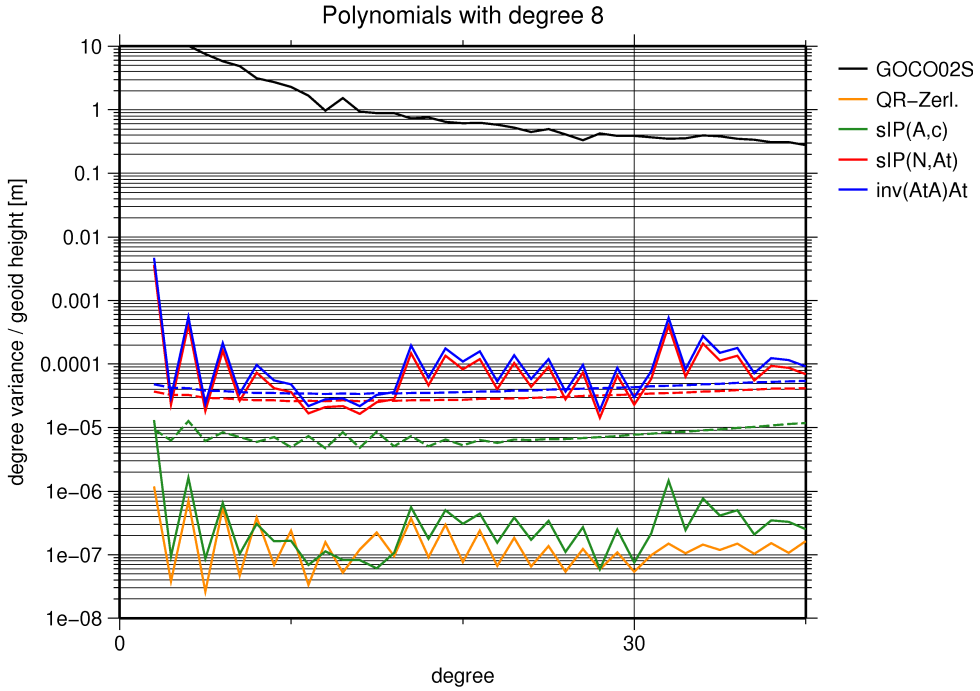

Figure 4: Degree variances with polynomial degree 8. black: reference model GOCO02S, green: implementation a, blue: implementation b, red: implementation c, orange: implementation d.

Figure 4 shows the results of the implementations derived with a polynomial of degree 8 without overdetermination. Here the first differences between the results occur.

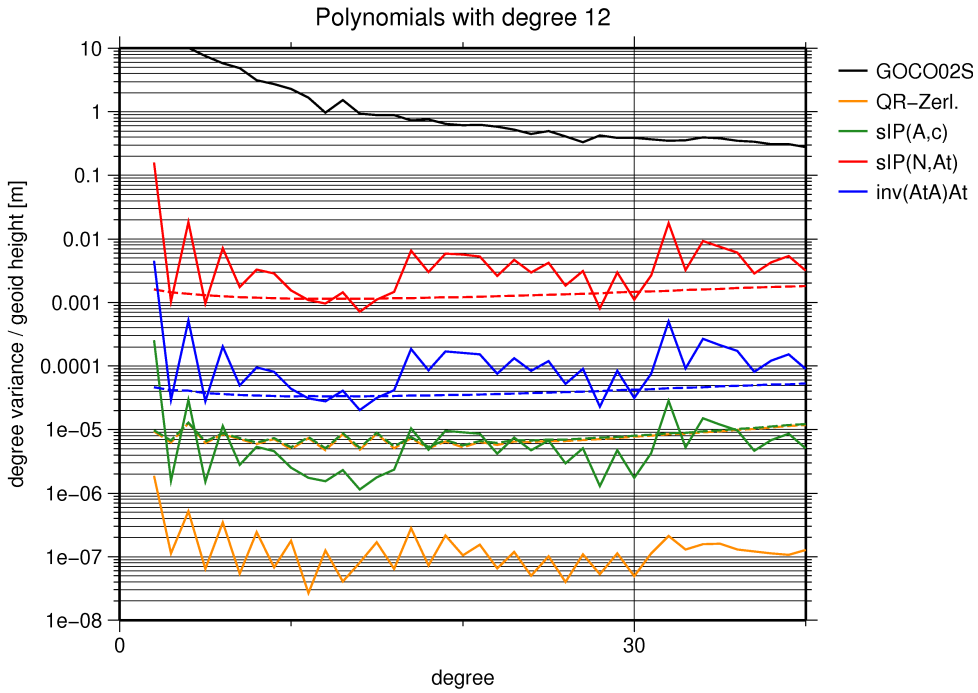

Figure 5: Degree variances with polynomial degree 12. black: reference model GOCO02S, green: implementation a, blue: implementation b, red: implementation c, orange: implementation d.

In Figure 5 the differences between the implementations are again bigger than in Figure 4. The used polynomial has degree 12. The only solution which still remains at an accuracy level of about 10^{-6} – 10^{-7} is the one using the QR decomposition. The other three solutions produce already numerical deviations in the filter which then influence the produced gravity field solution. Also noticeable is the fact that the three worst solutions show the same signature in the degree variances only scaled by a factor.

Summary

Looking at the results of the above presented simulations makes it clear that the fitting of the polynomial by means of the QR decomposition produces far the best results. If the simulation is continued to higher polynomial degrees the difference becomes even more obvious. The results of the QR decomposition stay at the same accuracy level whereas the other three implementations get worse and worse with every additional degree. Finally the effects of the errors in the filters become bigger than the desired results themselves. Due to this fact the QR decomposition will be used in the coming parts of the project.
But also the QR decomposition finally reaches its limits and produces numerically incorrect results. This is the case when the polynomial degree is increased to 34. These numeric problems are not immediately noticeable in the closed-loop simulations. The deviations are clearly visible when looking at the frequency response of the filter. At degree 34 no deviations are visible but at degree 36 the errors become obvious in the frequency response shown in Figure 6. An amplification of the signal takes place mainly in the high frequencies. With rising degree more and more frequencies are affected and the effect becomes stronger and stronger.

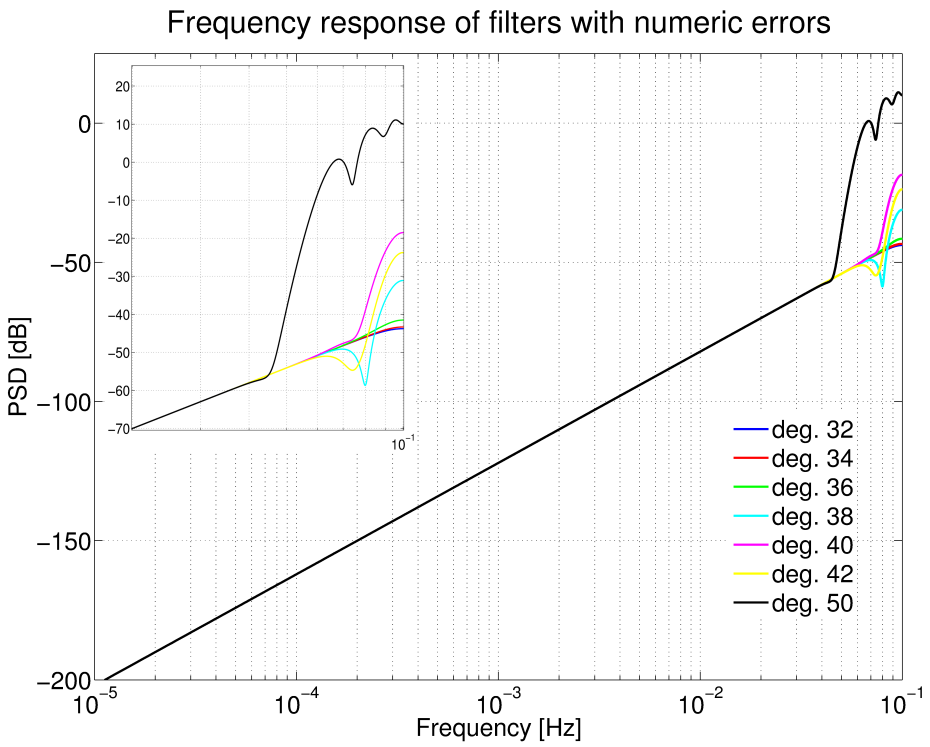

Figure 6: Frequency response of filters based on different polynomial degree from 32 to 50.

3.3 Outputs of WP 1

The results or outputs of this work package are the following:

- The best method for determination of accelerations has been found:
  - Polynomial interpolation.
- The best implementation of the polynomial interpolation has been found:
  - QR decomposition.
- This implementation has been integrated into the existing software package GROOPS:
  - Class ***podAcceleration.***
- The variance propagation for the polynomial interpolation has been set up.

4 WP 2 - Numerical studies

4.1 Inputs

The inputs for work package 2 are merely the outputs of work package 1. Which comprises the implemented software system and its modules for different tasks.

4.2 Tasks

Work package 2 comprises the testing of the implementation found in work package 1. Therefore some test scenarios were accomplished to find the advantages and disadvantages of the acceleration approach. Another point was to find out what impact does a certain change in the settings have on the resulting gravity field? Therefore, different changeable parameters have been investigated. These mentioned investigations were done by closed-loop simulations. The idea behind closed-loop simulations is described in chapter 3.2.6 Numerical stability section Comparison of the four implementations. Two distinctions have to be made, whether a noise is applied to the simulated orbit or not. If no noise is applied the differences only come from the chosen constellations or computation methods. If noise is applied, different nearly realistic scenarios can be simulated to check the effects of certain parameters.
The following chapters deal with these mentioned closed-loop simulations and changing parameters. The changeable settings are:

- Degree of interpolation or approximation polynomial.
- Number of used epochs and therefore the extent of overdetermination.
- Arc length.
- Sampling of the orbit data.
- Standard deviation of simulated orbit.
- Degree and order of the gravity field.

The basis for all simulations is the following in Table 4 described simulated orbit:

Parameter	Value
Semi-major axis	6621000 m
Eccentricity	0.0001
Inclination	89.9999 °
Ascending node	0 °
Argument of perigee	0 °
Mean anomaly	0 °
Degree and order of the gravity field	0 - 100
Reference gravity field	GOCO02S [11]
Starting time	01.01.2010 0:00:00
Ending time	01.02.2010 0:00:00
Sampling	1 sec

Table 4: Satellite constellation for WP 2 - Numerical studies.

This simulated orbit is the basis for all further investigations. For the different scenarios a noise is applied or the sampling is reduced. These settings are then mentioned explicitly for each scenario.

4.2.1 Implementation of noise-free scenario

The part of work package 1 Numerical stability described in chapter 3.2.6 was based on closed-loop simulations without adding noise to the simulated orbit. This corresponds to the work flow of a noise-free scenario. Therefore Figure 3, Figure 4 and Figure 5 show the results of a noise-free scenario. The results prove that when using the QR-implementation the whole software is working properly. The remaining differences in degree variance shown as geoid height which are in the range of 10^{-7}–10^{-6} meter come from the chosen constellation and the relatively short time span. Because of the mentioned simulations no separate noise-free scenario was implemented.

4.2.2 Implementation of noisy scenario & Comparison of derived satellite accelerations

Polynomials of different degree

The studies of work package 1 showed that the polynomial interpolation kernel is identical to the ones delivered by the Newton-Gregory or the Taylor-MacLaurin method. Furthermore they showed that the implementation using the QR decomposition is numerically the most stable one up to degree 34.

First the behavior of polynomials with varying degree have been investigated. In this case no overdetermination is introduced. This means that a polynomial with degree 8 uses 9 epochs to compute the accelerations and with degree 20, 21 observations are necessary. The results for different polynomials with degree 2 up to 20 are displayed in Figure 7. The simulation is based upon the previously described standard orbit, only a white noise with standard deviation of 2 cm is applied and the sampling is reduced to 5 seconds.

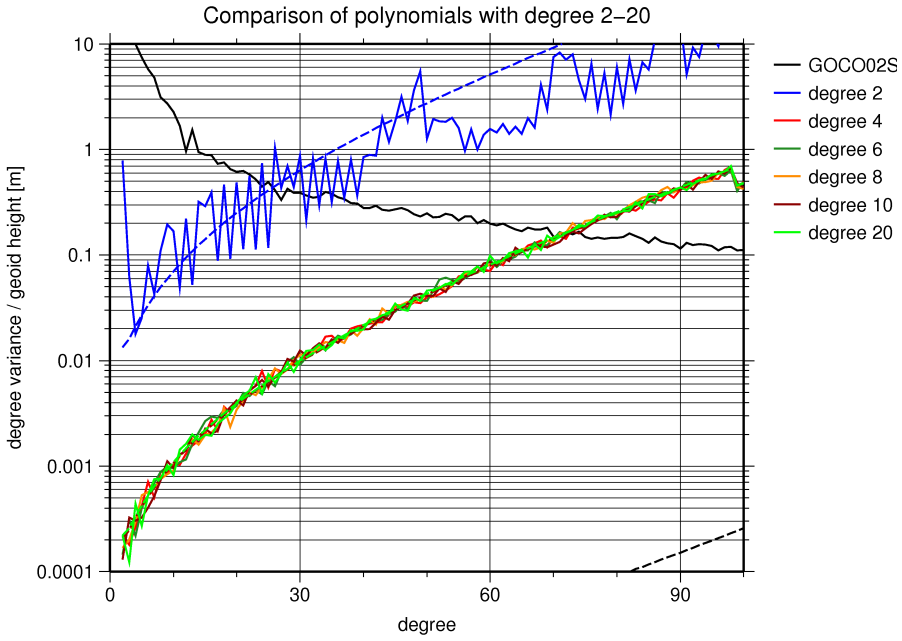

Figure 7: Differences in degree variance of solutions using polynomials with varying degree compared to the reference model GOCO02S. Degree 2 (blue), 4 (red), 6 (green), 8 (orange), 10 (brown), 20 (light green).

Figure 7 shows clearly that polynomials with a degree of 4 or higher provide almost the same results. Differences seen in the plot are only random and not significantly. Solely the gravity field estimated with a polynomial of degree 2 has bigger differences compared to the reference field. The polynomial with degree 2 is a special case. The used filter for deriving the accelerations represents the same operator as it is used in the acceleration approach using double differences or also called the 3-point scheme. This operator represents nothing more than a weighted mean of the three contributing observations. As already shown by Ditmar et. al. [5] this approach needs an additional weighting of the observations to get better results because the derived acceleration is an average over the time span of three observations. Therefore it is not valid for an explicit time any more.

All in all the degree of the polynomial has no or only a very small effect on the resulting gravity field model. The only disadvantage of a higher polynomial is the fact that when more observations contribute to the computation of the accelerations more data points get lost at the beginning and at the end of each arc.

Polynomials with overdetermination

If an overdetermination is introduced, more than degree + 1 observations are used to compute the accelerations. Therefore it is not an interpolation polynomial but an approximation polynomial. This causes a smoothing of the signal and higher Frequencies are damped. The goal of such a filter process is to reduce the noise in the data set to improve the gained gravity field solution. But if the filter is not chosen correctly, high frequency gravity field information is partially filtered. As a result these frequencies are also removed from the gravity field model. For the following studies the simulated orbit has been reduced to 5 seconds sampling and a positioning noise with standard deviation of 2 cm has been added.

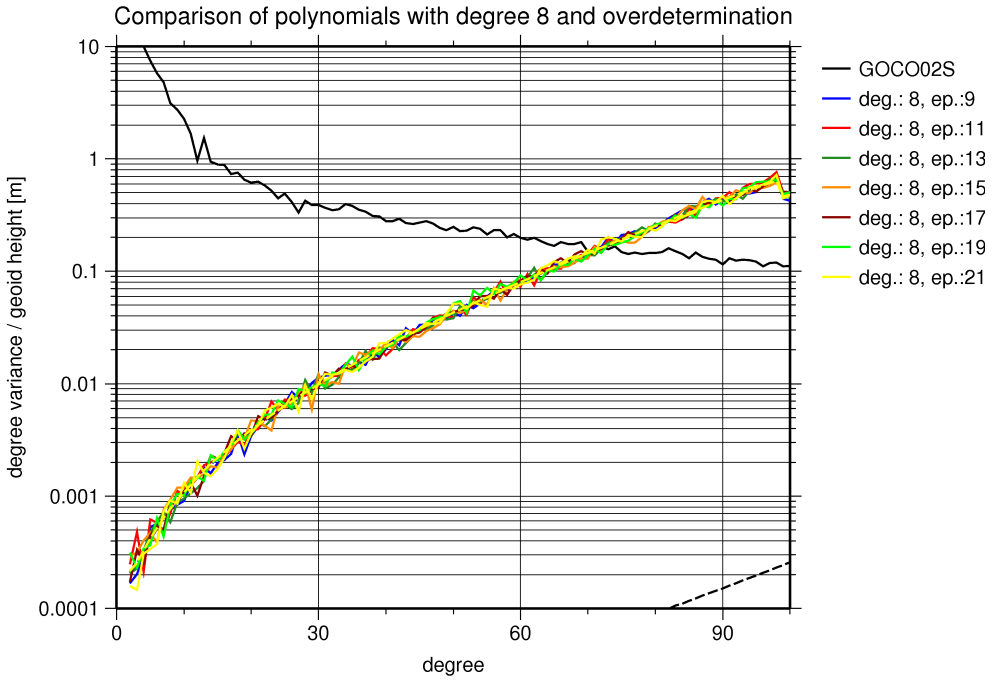

Figure 8: Difference in degree variance of solutions using polynomials of degree 8 with varying overdetermination compared to the reference model GOCO02S. Black: reference model GOCO02S. overdetermination 0 (blue), 2 (red), 4 (green), 6 (orange), 8 (brown), 10 (light green), 12 (yellow).

The constellations displayed in Figure 8 show very small differences with respect to each other. In general the results are identical and no damping effects can be seen. The applied polynomials have no effect, because the frequencies which are influenced by the filter process lie clearly above the maximum frequency represented by a gravity field of degree and order 100.

Because no differences can be seen in Figure 8 additional investigations have been carried out with polynomials of higher degree and with a greater overdetermination. The results are shown in Figure 9 and Figure 10.

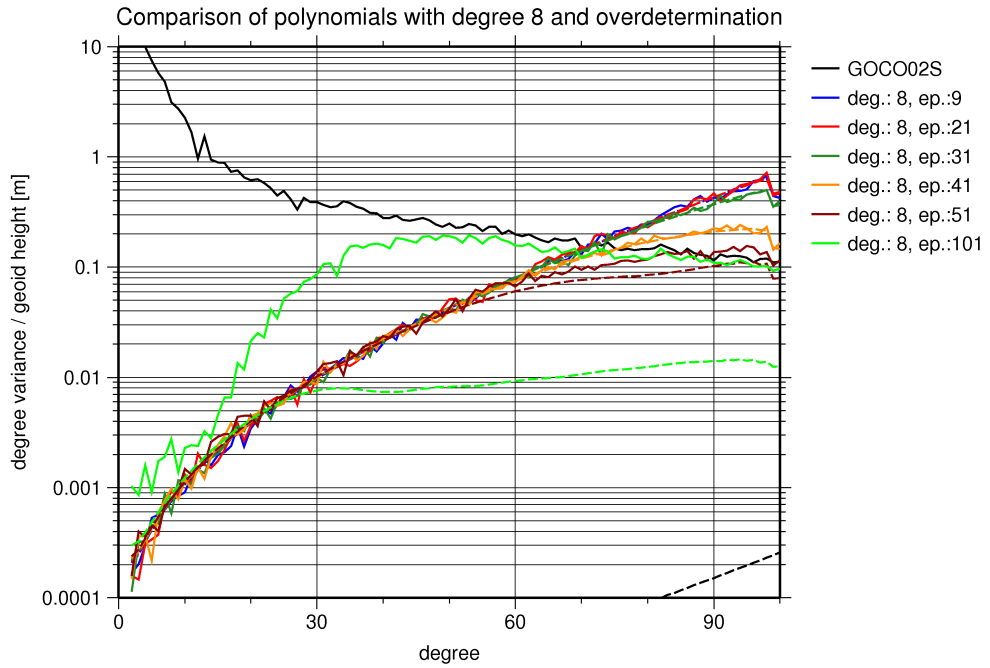

Figure 9: Difference in degree variance of solutions using polynomials of degree 8 with high overdetermination compared to the reference model GOCO02S. Black: reference model GOCO02S. overdetermination: 0 (blue), 12 (red), 22 (green), 32 (orange), 42 (brown), 92 (light green).

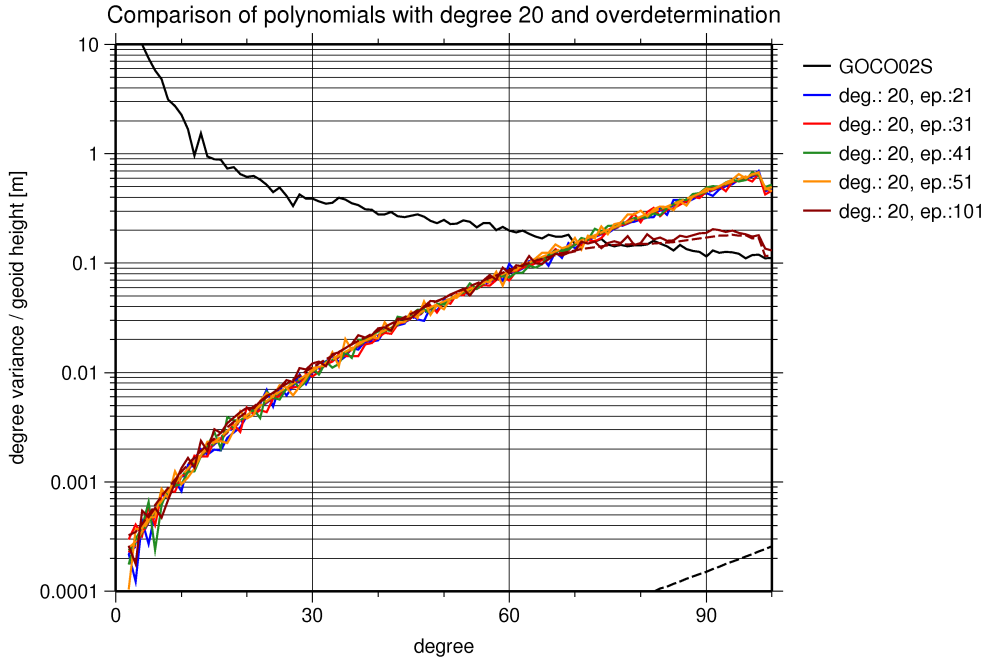

Figure 10: Difference in degree variance of solutions using polynomials of degree 20 with varying overdetermination compared to the reference model GOCO02S. Black: reference model GOCO02S, overdetermination: 0 (blue), 10 (red), 20 (green), 30 (orange), 80 (brown).

Figure 9 shows that with rising overdetermination in high degrees the results are getting better because noise is filtered out. But when the filter effect gets too strong it worsens the results in the lower degrees. The effect is getting stronger when the overdetermination gets larger. This is due to the fact that the filter reduces the influence of the noise on the

solution. But as seen in Figure 9 filtering the signal to strictly results in a worsening of the outcome because also signal gets filtered out.

From the two shown figures the following conclusion can be drawn: the bigger the over-determination of the polynomial the stronger is the filter effect. If the overdetermination is too large, the results get worse in the lower degrees because also signal is filtered out of the data set which contains the gravity field information. Additionally the estimated error is far away from the truth and is therefore not meaningful. The limits of filtering depend on degree and order of the estimated gravity field, the degree of the polynomial and the amount of overdetermination introduced to the polynomial.

When looking at the frequency spectrum of the used polynomials especially the frequency response of the corresponding filter, the above described problems and conditions can be displayed very clearly.

The following figures show the frequency response of different filters. Additionally some important frequencies are marked to facilitate the interpretation of the results.

First of all, let us look at the power spectral density of the simulated orbit positions, velocities and accelerations. The X component is displayed in Figure 11.

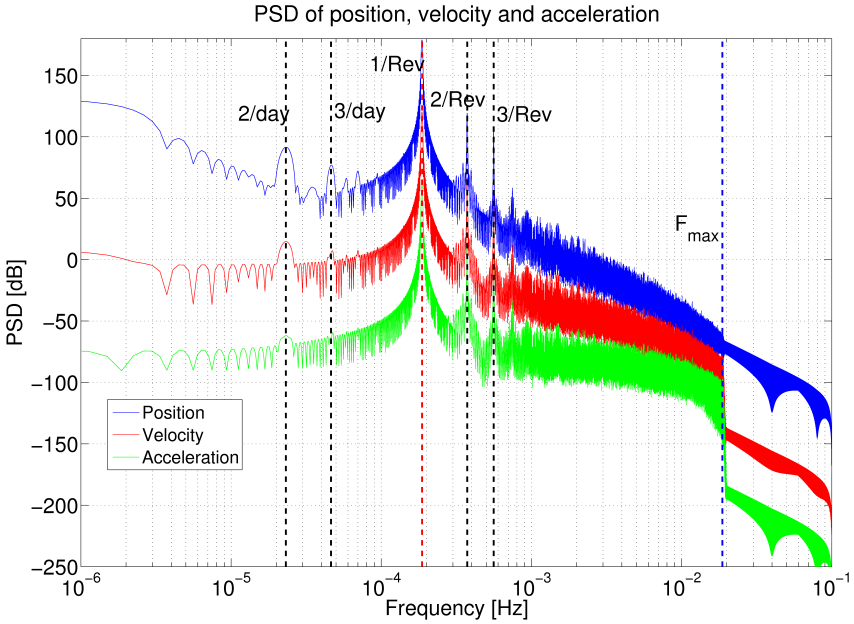

Figure 11: Power spectral density of positions (blue), velocities (red) and accelerations (green) and a few important frequencies.

In Figure 11 it can be clearly seen that there is a dramatic decrease in signal strength from positions to velocities and then again to accelerations. But the frequency response stays alike in all three cases. Some important frequencies can be seen clearly, like the frequencies 2/day, 3/day, 4/day, ... and these connected to the orbital period, like 1/revolution, 2/revolution, ... Also the maximum frequency of the used gravity field for simulating the orbit is clearly visible. The degree of a gravity field can be converted into a frequency with the following formula

$$f_{max} = \frac{l_{max}(N_r N_d)}{(N_d N_t)}.$$

f_{max}	...	maximum frequency	
l_{max}	...	degree/order of the gravity field	(4.1)
N_r	...	number of revolutions per day	
N_d	...	number of operating days	
N_t	...	number of seconds per day	

The frequencies above the maximum contain no information. This is indicated by the immediate loss of signal strength above the chosen frequency maximum. Looking at the same representation for an orbit when white noise is added and the accelerations are derived by means of numerical differentiation, gives the following figure:

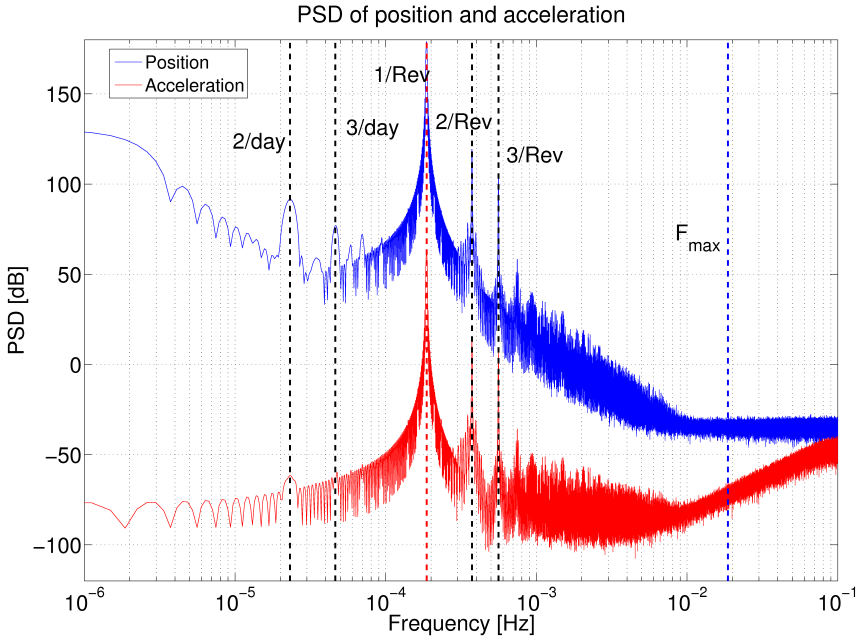

Figure 12: Power spectral density of positions (blue) and accelerations (red) with 2cm white noise and a few important frequencies.

The orbit used here has a white noise with 2 cm standard deviation added. Afterwards the accelerations were produced using polynomial interpolation with a polynomial of degree 8 without overdetermination. In general the signals show the same behavior as the signals without noise. But starting from a frequency of approximately 0.007-0.008 Hz noise exceeds the signal itself. In the power spectral density of the positions it can be seen that the noise with 2 cm standard deviation has an amplitude of about -35 dB in the single frequencies. By differentiating the signal the high frequencies are getting amplified. This is visible in the power spectral density of the derived accelerations.

When using overdetermined polynomials high frequencies are attenuated. Depending on the degree and the amount of overdetermination a different number of frequencies is affected. In principle the following rules are valid:

- The higher the degree of the polynomial the narrower the frequency range which is affected.

- The higher the overdetermination the wider is the affected frequency range.

Based on these basic rules, different filters can be designed according to the desired properties. Another feature of the filters is the fact that in the frequency range which is affected, some frequencies are almost eliminated. The number of these nearly removed frequencies depends on the overdetermination of the used polynomial.

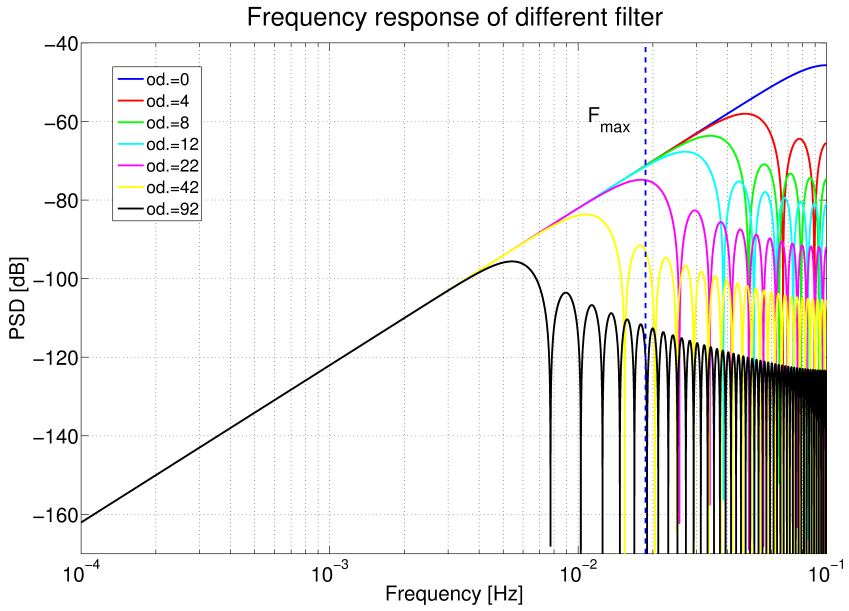

Figure 13: Frequency response of filters with degree 8 and an overdetermination of 0 (blue), 4 (red), 8 (green), 12 (cyan), 22 (magenta), 42 (yellow) and 92 (black).

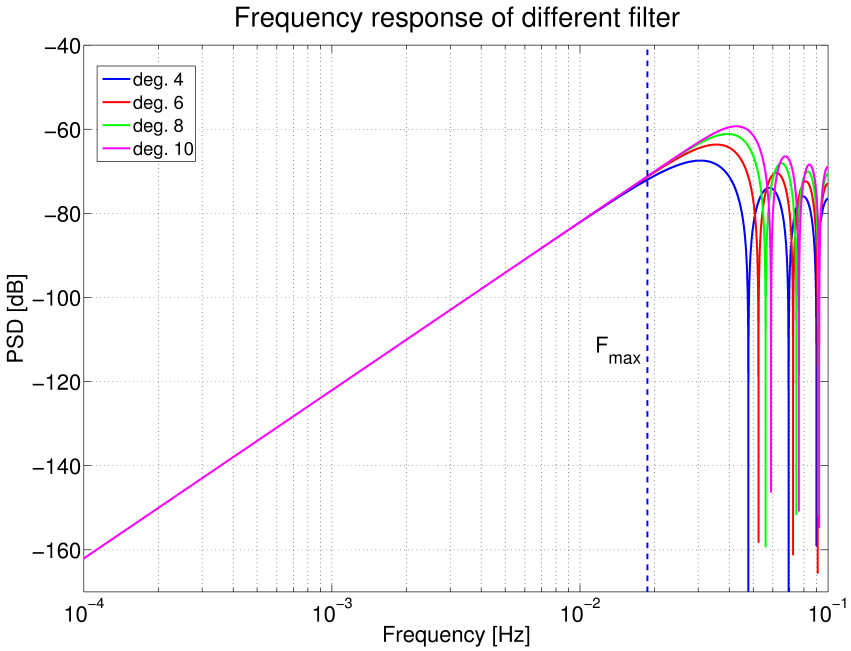

Figure 14: Frequency response of filters with degree 4 (blue), 6 (red), 8 (green) and 10 (magenta) and an overdetermination of 6.

Figure 13 shows the rising number of damped frequencies and the wider range of affected frequencies when the overdetermination is getting higher. The used polynomial was of degree 8. Figure 14 shows filters with different polynomial degree but the same overdetermination. Here we can see that with higher degree the range of affected frequencies gets smaller and smaller. The frequency response of the filter is also visible in the power spectral density of the residuals.
Figure 15 shows a few examples.

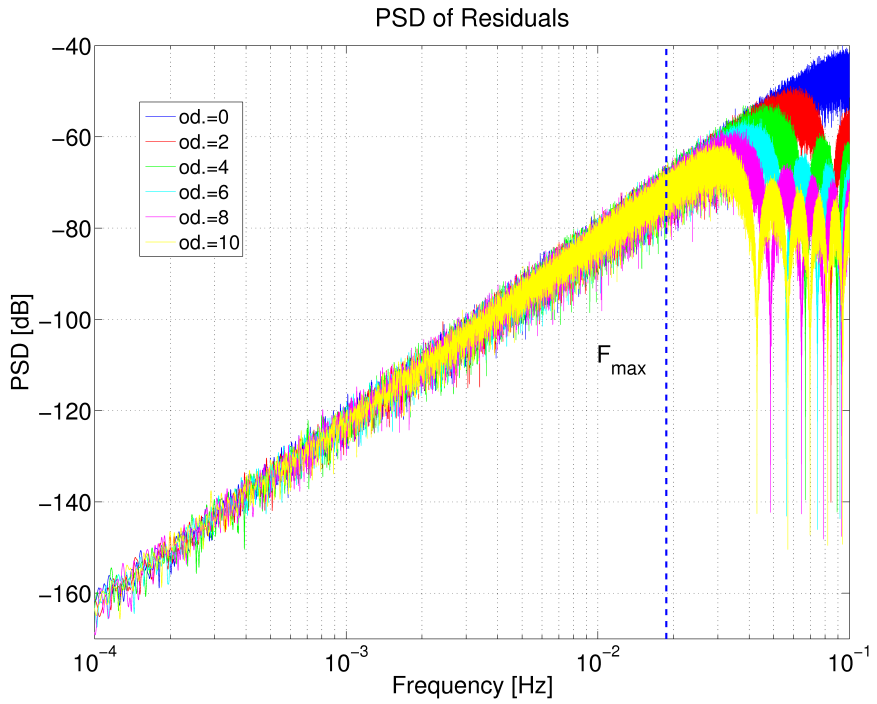

Figure 15: Power spectral density of acceleration residuals produced with polynomials of degree 8 and an overdetermination of 0 (blue), 2 (red), 4 (green), 6 (cyan), 8 (magenta) and 10 (yellow).

The structure of the filters frequency response is clearly visible. The eliminated frequencies can be seen as well as the width of the affected range. If we look at the effects which the displayed filters have on the final result in terms of a gravity field model, no impact at all is recognizable as seen in Figure 8. This is due to the fact that none of the used configurations has an effect on frequencies below the maximum frequency of the estimated gravity field.
But when using filters which have an effect on frequencies below the maximum frequency of the gravity field, this is also seen in the gravity field solution. Figure 16 shows the power spectral density of residuals computed with different filter designs. Comparing this plot with Figure 9 makes the connection obvious. Starting from an overdetermination of 32 the filter causes changes in the frequencies below the maximum frequency. In the solution the difference between estimated solution and “true” reference field gets smaller. But this improvement is not very useful because the difference between reference and estimation is

still bigger than the signal itself. If a polynomial with a too strong filter effect is used the solution becomes unstable. In Figure 16 it can be seen that the yellow data set of residuals obviously still contains some signal.

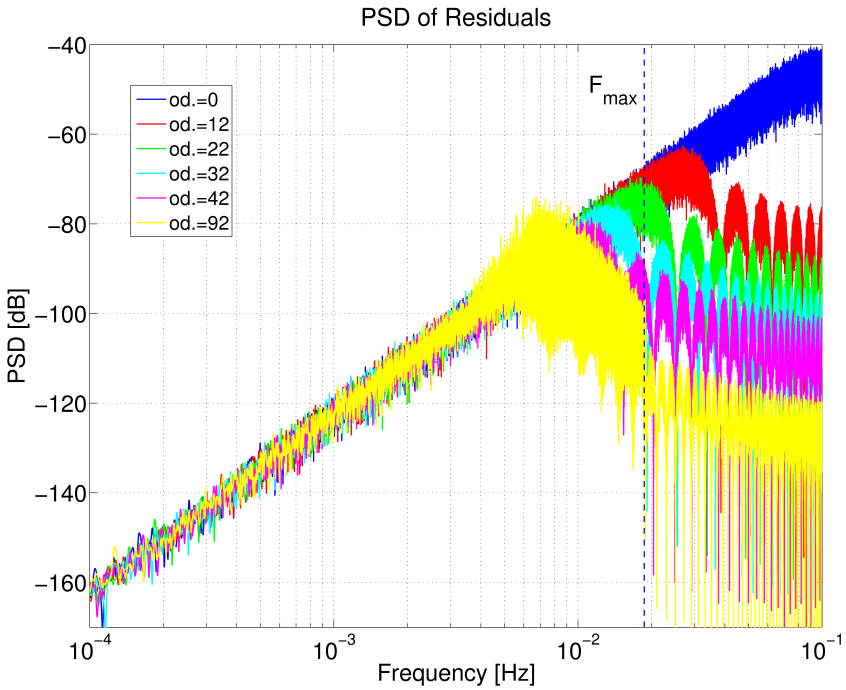

Figure 16: Power spectral density of acceleration residuals produced with polynomials of degree 8 and an overdetermination of 0 (blue), 12 (red), 22 (green), 32 (cyan), 42 (magenta) and 92 (yellow).

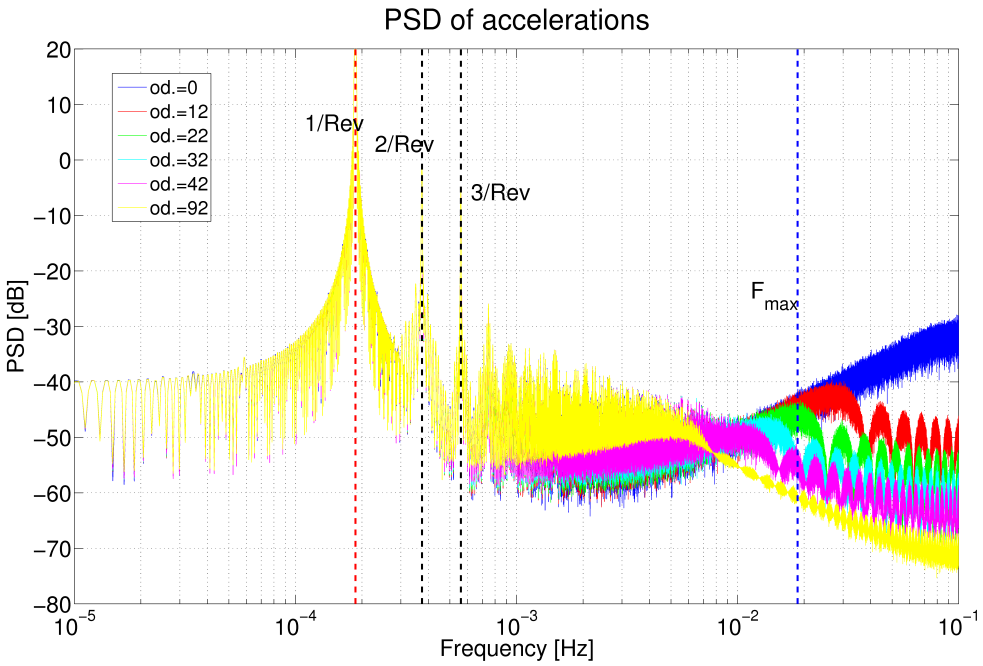

Figure 17: Power spectral density of accelerations derived with polynomials of degree 8 and with an overdetermination of 0 (blue), 12 (red), 22 (green), 32 (cyan), 42 (magenta) and 92 (yellow).

In Figure 17, the attenuation of the high frequencies in case of overdetermined filters is clearly visible. But when this attenuation affects frequencies below the maximum frequency of the gravity field, the resulting gravity field model becomes erroneous.
Another problem in case of a too strong filtering is the fact that the error estimation becomes too optimistic and is way below the true errors and therefore gives a misleading information.

Using different sampling

The simulated orbit has a sampling of 1 second. In many cases it is useful and sufficient to use a lower sampling rate. Lower sampling means less data and as a consequence it means faster computing times. But by reducing the amount of data, the result also gets worse. To get an impression of the effects of a higher or lower sampling a few different scenarios were simulated. As the number of epochs per arc vary they have a different number of epochs but the same length in terms of time which can also have effects on the quality of the solution.

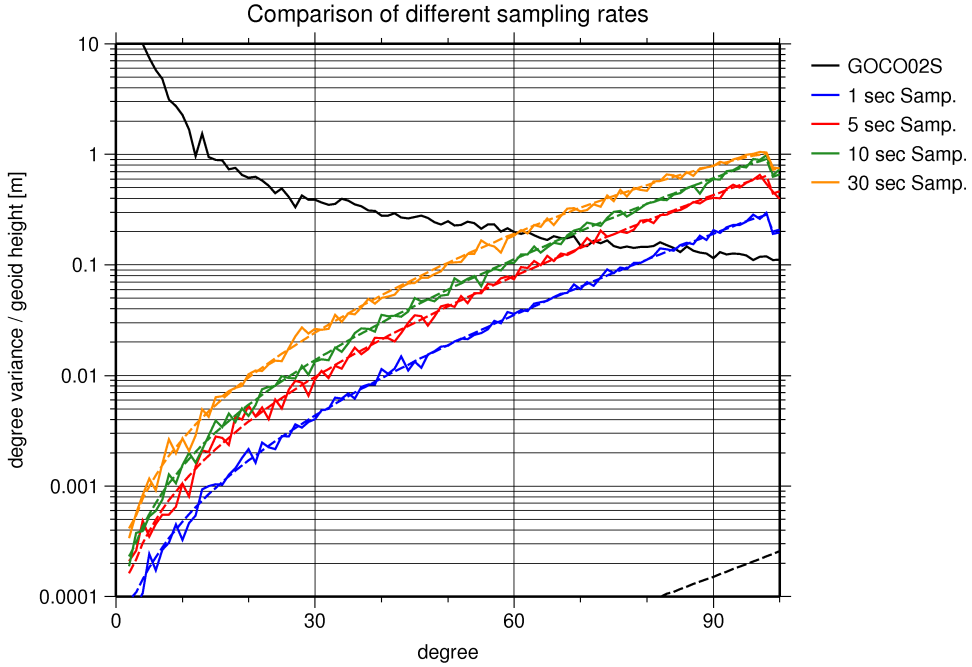

Figure 18: Differences in degree variance of results using different sampling compared to the reference model GOCO02S. Black: reference model GOCO02S. Used sampling: 1 second (blue), 5 seconds (red), 10 seconds (green), 30 seconds (orange).

The comparison in Figure 18 shows that when reducing the sampling rate the quality of the solution decreases. The reason for this is simply the reduced amount of data. Otherwise there is no negative impact on the results. Additionally the portion of lost data points at the beginning and the end of an arc also increases with lower sampling and constant arc length.

Using different arc lengths

Another parameter which can affect the quality of the estimated gravity field is the arc length. The used orbit data is cut into several pieces called arcs. This is particularly due to computational reasons to make the assembling of the normal equations faster. To do this the assumption is made that the single arc are independent from each other and no correlations exist between them. This is not exactly true because neighboring positions are correlated. Therefore the arc length has an impact on the quality of the results. The length should be chosen in a manner that it exceeds the correlation length of the positions in time but nevertheless the computational burden should not get too large. If the arc length is chosen too short it affects mainly the low degrees in the gravity field.
Figure 19 shows the effects of different arc lengths on the resulting solution. Short arcs with a length of 5 or 10 minutes produce worse quality in the low degrees. Arcs with a duration of 20 or more minutes show all the same level of accuracy. When using the same sampling the portion of lost data points due to the filtering is higher for short arcs and therefore it additionally reduces the quality of the estimation.

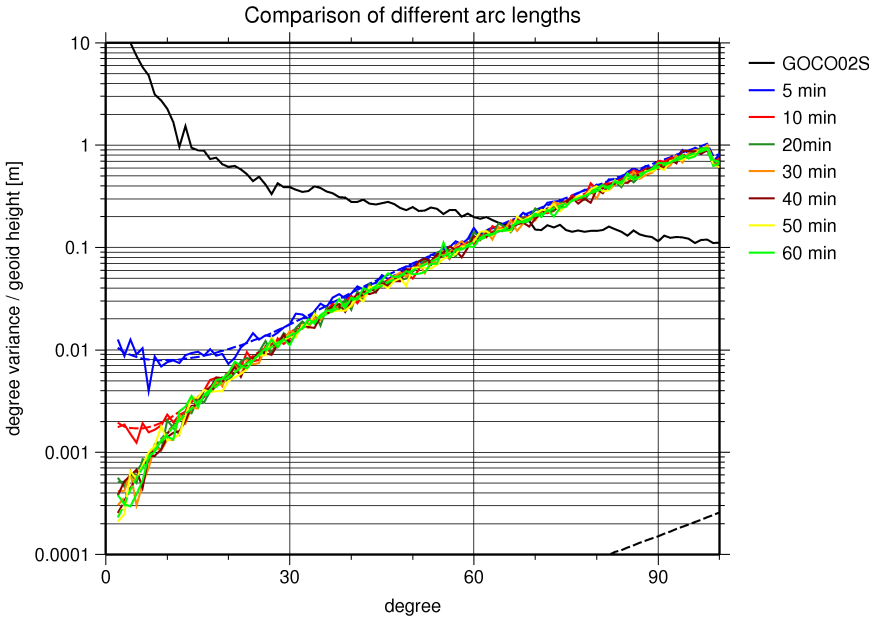

Figure 19: Differences in degree variance of results using different arc lengths compared to the reference model GOCO02S. Black: reference model GOCO02S. Used arc length: 5 minutes (blue), 10 minutes (red), 20 minutes (green), 30 minutes (orange), 40 minutes (brown), 50 minutes (yellow) and 60 minutes (light green).

4.2.3 Quality assessment

Based on the results of the previously shown investigations some assumptions about the implemented acceleration approach and its quality can be made.

- The implemented software works correct.
- The used polynomial interpolation comprises all other methods.
- Changing the polynomial degree has nearly no effect on the results.
  - Except for degree 2, which represents a special case.
- Using overdetermination brings nearly no advantages.
- Too high overdetermination results in a decrease of the achieved accuracy.
- Data sampling affects the solution as more or less observations are used.
- Arc length should be greater than 20 minutes.

If the mentioned facts are kept in mind a solution with sufficient accuracy can be obtained solely depending on the used satellite constellation, the observation quality and the available amount of data.

4.3 Outputs of WP 2

Work package 2 has several outputs which are the basis for the upcoming work packages. The completion of the software testing in a suitable test environment was reached. In accordance with the previous chapters and based on the gained insights a polynomial interpolation with degree 8 and no overdetermination is chosen as the baseline differentiator. This choice is based on the facts that overdetermination brings no benefits, the degree is not very important and with a length of 9 epochs the loss of data points is manageable. Last but not least the midterm report was finished in the frame of work package 2.

5 WP 3 - Gravity field processing

5.1 Inputs

Starting point for work package three are the results of work package 1 and 2. This comprises the implemented software as well as the defined baseline differentiator. Additionally, some models of different influences, for example different tide models to compensate their influence on the measurements, are necessary. One important input is the orbit, attitude and accelerometer data of the used satellites. The computation of various gravity fields is based on these inputs.

In detail the inputs are the following:

Type	Description
Software	GROOPS and the implemented modules for the acceleration approach
Baseline differentiator	Polynomial interpolation with degree 8 and no overdetermination
Models	DE405 JPL planetary ephemeris (direct tides)
	Earth tides according to IERS convention
	Empirical Ocean Tide Model 2011 (EOT11a)
	Pole tide model
	Grace Atmosphere and Ocean Dealiasing (AOD1B): short term variations in atmosphere and ocean
Satellite data	Orbit positions, variance information of orbit positions, star camera data, accelerometer data. Used satellite missions: CHAMP and GOCE

Table 5: List of input data used for gravity field processing.

5.2 Tasks

5.2.1 Formulation of functional and stochastic model

The connection between accelerations and the gravity field is in principle described in section 3.1.1 Gravity field determination using orbit information and 3.2.1 Algorithm design. The therein described equations are now used to set up the whole system of equations and then to estimated the desired parameters by means of a least squares adjustment.
All observations are combined in a vector l. This vector can be described by the model $M(x)$ and the random errors e. This leads to the model of linear equations

$$l = M(x) + e\,. \tag{5.1}$$

In most cases the model is not linear and therefore has to be linearized. This is done by forming a Taylor series of the model and truncating it after the linear term. In general the computation should start with the introduction of an approximate solution for the desired parameters

$$l = l(0) + \frac{\delta M(x)}{\delta x}\Big|_0 (x - x_0) + \dots \,. \tag{5.2}$$

The observations are reduced for the approximation, the partial derivatives are combined in the design matrix and supplements to the parameters are defined. This yields the following system of linear equations

$$l = Ax + e \,. \tag{5.3}$$

This system is solved through least squares adjustment which leads to the system of normal equations

$$\boldsymbol{N}\hat{\boldsymbol{x}} = \boldsymbol{n} \quad \boldsymbol{N} = \boldsymbol{A}^T \boldsymbol{P} \boldsymbol{A} \;\text{ and }\; \boldsymbol{n} = \boldsymbol{A}^T \boldsymbol{P} \boldsymbol{l} \,. \tag{5.4}$$

Where $\boldsymbol{P}$ is the weight matrix, derived from the covariance information of the orbit positions respectively the accelerations. This now leads to the estimated parameters and their covariance matrix

$$\hat{\boldsymbol{x}} = \boldsymbol{N}^{-1}\boldsymbol{n} \quad \text{and} \quad \boldsymbol{C}(\hat{\boldsymbol{x}}) = \sigma^2 \boldsymbol{N}^{-1} \,. \tag{5.5}$$

5.2.2 Assembling of pseudo observations and the system of equations

Building the system of equations for a big data set soon becomes very expensive in terms of computational burden. Let us consider one month of observation data with a sampling of 1 s. This leads to a total of approximately 2.6 million observations. Each observation consists of 3 coordinates or accelerations in case of SST-hl. So all in all 7.7 million equations have to be set up. On the other hand the number of parameters depends on the maximum degree and order to which the gravity field is estimated. For example when using degree and order 150, a total of 22801 parameters have to be found. Assuming double precision using a 32 bit machine leads to a desired storage of about 650 GB for the design matrix and 215 TB for the covariance matrix of observations if fully occupied. This would be far to big for any average PC. This amount of data would also bring an actual supercomputer to his edges. Therefore special computational methods are implemented to reduce the necessary computing time.

The software GROOPS is based on the short arc approach. This means the whole data set is split into short arcs with a length of a few minutes. Investigations showed that the minimum length should be greater than 15-20 minutes. The system of equations, the

design matrix, the observations vector and the weight matrix of observations, is built up for every arc separately. Afterwards, they can be combined to form the whole system

$$\boldsymbol{l}=\begin{pmatrix}\boldsymbol{l}_1\\ \boldsymbol{l}_2\\ \cdot\\ \cdot\\ \cdot\\ \boldsymbol{l}_m\end{pmatrix} \quad \text{and} \quad \boldsymbol{A}=\begin{pmatrix}\boldsymbol{A}_1\\ \boldsymbol{A}_2\\ \cdot\\ \cdot\\ \cdot\\ \boldsymbol{A}_m\end{pmatrix} \quad \text{and} \quad \boldsymbol{P}=\begin{pmatrix}\boldsymbol{P}_1 & & & \\ & \boldsymbol{P}_2 & & \\ & & \ldots & \\ & & & \boldsymbol{P}_m\end{pmatrix}. \tag{5.6}$$

The combination of the matrices $\boldsymbol{P}_i$ to form a block diagonal matrix is only valid if the blocks are not correlated. If this is the case, the normal equations can be built up for each block and then summed up.

$$\boldsymbol{N}=\sum_{i=1}^{m}\boldsymbol{A}_i^T\boldsymbol{P}_i\boldsymbol{A}_i \quad \text{and} \quad \boldsymbol{n}=\sum_{i=1}^{m}\boldsymbol{A}_i^T\boldsymbol{P}_i\boldsymbol{l}_i\,. \tag{5.7}$$

In general the used positions are correlated over time. So the weight matrix $\boldsymbol{P}$ won't be block diagonal. To get a block diagonal structure the individual parts are decorrelated. This is done by a cholesky decomposition. Furthermore the correlations between different blocks are neglected, due to the fact that they are very small and would have no influence on the solution. This is true if the length of the arc is 15 minutes or greater as the tests shown under section 4.2.2 Implementation of noisy scenario & Comparison of derived satellite accelerations showed.

$$\boldsymbol{P}^{-1}=\boldsymbol{W}^T\boldsymbol{W} \tag{5.8}$$

The matrix $\boldsymbol{W}$ is an upper triangular matrix. To get the inverse of $\boldsymbol{P}$ $\boldsymbol{W}$ is inverted. But this inversion is done by backward substitution and is therefore faster than computing directly $\boldsymbol{P}^{-1}$. Now the equation 5.8 is inserted into formula 5.7 which leads to

$$\begin{aligned}\bar{\boldsymbol{A}}&=\boldsymbol{W}^{-T}\boldsymbol{A} \quad \text{and} \quad \bar{\boldsymbol{l}}=\boldsymbol{W}^{-T}\boldsymbol{l}\\ \boldsymbol{N}&=\bar{\boldsymbol{A}}^T\bar{\boldsymbol{A}} \quad \text{and} \quad \boldsymbol{n}=\bar{\boldsymbol{A}}^T\bar{\boldsymbol{l}}\end{aligned}\,. \tag{5.9}$$

This transformation is called decorrelation or homogenization. Formal it leads to an estimate based on uncorrelated observations with equal variance. This decorrelation is done for every single arc. The correlations between the different arcs are neglected. As already mentioned above, this can be done because the correlation between two positions is converging to zero with increasing time difference.

This approach not only has the benefit that the matrices built up are kept small and therefore the computational burden is acceptable. Additionally it is also best suited for parallelization on a multi-core environment or a PC cluster. Each available processor can handle a single arc and submit his results to the master processor. The master only has to sum up all normal equations and then solve the system of equations.

Variance component estimation

As already mentioned before the orbit positions are split into short arcs during the processing and normal equations are built for each arc separately. The observations are weighted according to their variance but this approach also gives the possibility to use a different weight for each arc. The same approach can also be applied to the combination of individual monthly normal equations. For example when combining CHAMP and GOCE observations because these two missions feature different accuracies and characteristics. The used approach for estimating the individual variances, respectively weights, is based on the so called variance component estimation as described by *Koch and Kusche* [15]. The core aspect of this approach is to build up the whole system of normal equations from a set of individual normal equations

$$\boldsymbol{N}\hat{\boldsymbol{x}}=\boldsymbol{n} \quad \text{where} \quad \boldsymbol{N}=\sum_k \frac{1}{\hat{\sigma}_k^2}\boldsymbol{N}_k \quad \text{and} \quad \boldsymbol{n}=\sum_k \frac{1}{\hat{\sigma}_k^2}\boldsymbol{n}_k . \tag{5.10}$$

The weight is determined by the reciprocal of the variance for each normal equation

$$\hat{\sigma}_k^2=\frac{\Omega_k}{r_k} . \tag{5.11}$$

Where the squared sum of residuals is given by

$$\Omega_k = \hat{\boldsymbol{e}}_k^T\hat{\boldsymbol{e}}_k = (\boldsymbol{A}_k\hat{x}-\boldsymbol{l}_k)^T(\boldsymbol{A}_k\hat{x}-\boldsymbol{l}_k) \tag{5.12}$$

and the partial redundancy of this group of observations is

$$r_k = m_k - \frac{1}{\sigma_k^2}trace(\boldsymbol{N}_k\boldsymbol{N}^{-1}) \tag{5.13}$$

where m_k is the number of observations for this group. If all partial redundancies are summed up they lead to the overall redundancy

$$\sum_k r_k = m-n . \tag{5.14}$$

m ... number of observations
n ... number of parameters

For the computation of the variances the solution and also the individual variances are necessary. Due to this fact the computation of the solution must be carried out iteratively. This means the newly estimated variances are introduced into equation 5.10. This iteration is carried out several times until a abort condition is fulfilled. This can be realized by a fixed number of iterations or the repetition is stop if the change in the total variance is below a defined threshold.

5.2.3 Estimating gravity fields

The core task of work package 3 is to use real observation data to generate different types of gravity fields. As mentioned before the used data comes from the two satellite missions CHAMP and GOCE. The following table shows the work flow for processing the data.

Step	*Description*
Data import	Read data from the proprietary formats of the satellite mission and save it in GROOPS internal formats. Used data sets: • Orbit positions • Variances and covariances of orbit positions • Star camera data • Accelerometer data Furthermore, the data was combined to monthly data sets.
Data sampling	The available data sets have a nearly constant sampling, but for the numerical differentiation a constant sampling is necessary. So they were brought to a constant sampling by interpolation.
Data reduction	In case of GOCE the data has a sampling of 1 Hz. To reduce the amount of data for some applications only every fifth or tenth data point is used.
Designing arcs	The whole data set is cut into arcs with a maximum length which can be defined. But when there is a data gap the actual arc must be ended and the next begins. Therefore also a minimum arc length must be defined, to avoid arcs which are only a few seconds long. • Minimum: 15-20 min • Maximum length 45-60 min
Empirical covariance function	The provided orbit covariance information contains only variances and covariances for every single epoch. Between different epochs no covariance information is available. Therefore an empirical covariance function has to be found. This is done on basis of orbit residuals with respect to a static gravity field. This function is then used in combination with the variance information for every position to build up the weight matrix.
Build normal equations	According to the described algorithm the normal equations are build. After combination of all blocks the result is saved to a file so that it can be used again later.
Solve system of equations	The normal equations are solved according to the rules of least squares adjustment.
Potential coefficients	The estimated coefficients and an eventually subtracted reference field are combined and the resulting coefficients are saved.
Visualization	Plotting certain forms of the estimated gravity field, e.g. geoid height, degree variances, spherical harmonics triangle, ...

Table 6: Work flow for gravity field processing.

5.3 Outputs

Result of work package 3 is the completed software module for processing gravity fields by using the acceleration approach as well as some gravity field models based on real observation data.

5.3.1 Software modules

The implemented software modules comprise the necessary functionality for the acceleration approach. The mathematical background about the acceleration approach is already explained in detail in the section 3.1.1 Gravity field determination using orbit information. Now we take a look at the implementation of the method in the software package GROOPS.
The modules used to prepare the data, save the results or to plot them were already implemented in GROOPS and are not of interest at this point. The focus lies on the module which handles the setting up and accumulation of the system of normal equations.
This module comprises the class *observationPodAcceleration* and its member functions *observationPodAcceleration* and *observation.* These two functions are responsible for setting up the observation equations for each arc. The function *observationPodAcceleration* reads the input files and checks the chosen parameter settings. The function requires the following parameters:

- right hand side
  - input file orbit
  - input file accelerometer
  - reference field
  - tides
- input file orbit
- input file star camera
- earth rotation
- representation of gravity field as spherical harmonics
  - min degree
  - max degree
  - GM (3.986004415e+14)
  - R (6378136.3 m)
- interpolation degree
- number of epochs
- weighting: yes/no
- estimate accelerometer scale
- estimate accelerometer bias
- use covariance: yes/no
  - sigma

  - input file sigmas per arc
  - input file covariance per epoch (3x3 matrix for each epoch)
  - input file covariance function (use covariance function for correlations over time)
- maximum arc

The function *observation* is called for every arc separately and builds up the system of equations based on the imported data files and the chosen parameters. The equations are then returned back to the calling function *normalsBuild* which accumulates the results of all arcs to the final resulting system of equations.

Another important class is *CovariancePod*. It is responsible for handling the covariance information about the orbit positions. There are four different possibilities how this information can be provided. First one is to define a fixed value for the variance of all coordinate directions. This would lead to a covariance matrix with the chosen variance in its main diagonal. The second possibility is to define an individual sigma for each arc. This would also provide a covariance matrix with values only in the main diagonal, but different variances for each arc. The third possibility is to provide the 3x3 covariance matrices for each epoch which come from the processing of GPS observations. In this case the produced covariance matrix would have a block diagonal structure. The fourth method uses a given covariance function to account for the correlations in time. This leads to a full covariance matrix were also the off-diagonal elements are filled with the information of the covariance function. The four methods can be combined to get an optimal estimation of the covariance matrix. The ideal case would be to use the full covariance matrix which comes from the orbit estimation process. But in case of the GOCE and CHAMP data processing this information is not provided.

5.3.2 Gravity field models

Description of the used satellite missions

CHAMP

The CHAMP satellite was a German research satellite dedicated to the study of Earth's gravity and magnetic field as well as the atmosphere and the ionosphere. Launched on July 16, 2000, its mission end came on September 19, 2010. During 10 years of operations it collected a huge amount of data to investigate different aspects of the system earth. Its main scientific instrumentation is listed in Table 7.

Instrument	Manufacturer	Observations
STAR accelerometer	Centre National d'Etudes Spatial (CNES), France	Non-gravitational accelerations acting on the satellite
GPS receiver TRSR-2	NASA Jet Propulsion Laboratory, Passadena USA	GPS observations: code and phase measurements on L1 and L2
Laser Retro Reflector	Geoforschungszentrum (GFZ), Potsdam Germany	Passive instrument for satellite laser ranging
Fluxgate Magnetometer	Technical University of Denmark (DTU), Lyngby Denmark	Vector components of the earth's magnetic field
Overhauser Magnetometer	Laboratoire d'Electronique de Technologie et d'Instrumentation (LETI), Grenoble France	Scalar magnetic field
Advanced Stellar Compass	Technical University of Denmark (DTU), Lyngby Denmark	Attitude parameters
Digital Ion Drift Meter	Air Force Research Laboratory (AFRL), Hanscom USA	In-situ measurements of the ion distribution in the ionosphere

Table 7: CHAMP payload description.

For the processing of gravity field solutions in the present project orbit, accelerometer and attitude data is available for the time span January 1, 2002 till December 31, 2009. The kinematic orbit solutions are kindly provided by the University of Bern (AIUB) and have been previously used in the frame of the GOCO project to contribute to the two gravity field releases GOCO01S and GOCO02S. The associated accelerometer and star camera data is provided by the Information System and Data Center operated by the GFZ Potsdam.

GOCE

The GOCE satellite was build by the European Space Agency (ESA) as one of its Earth explorer missions in the frame of the living planet program. It was successfully launched on March 17, 2009. The main purpose if this mission is to map the static gravity field of the earth with an unrivaled accuracy. The main instrumentation consists of following parts listed in table 8.

Instrument	Manufacturer	Observations
Gravity gradiometer	Thales Alenia Space France and Office national d'études et recherches aérospatiales (ONERA), France	Accelerations acting on Gravity gradients
GPS receiver	Thales Genial Space Italia	GPS observations: code and phase measurements on L1 and L2
Laser Retro Reflector		Passive instrument for satellite laser ranging
Drag-Free and Attitude Control System	Several components	Maintained the orientation and compensates the atmospheric drag action on the satellite

Table 8: GOCE payload description.

The GOCE satellite has been delivering scientific data since November 2009 until now, except for some gaps. End of mission will come in 2013. In this project all presently available data sets have been used to generate monthly solutions of the gravity field and to produce a combined solution for the whole data set. The data set so far available spans from November 1, 2009 till July 31, 2011. The focus was on producing gravity fields from orbit data only to see the influences of different parameters on the estimation process.

Models

All in all three different types of gravity fields were produced. The coefficients of these models are provided on the website of the ITSG (www.itsg.tugraz.at). The used gfc file format is a quasi standard for exchange of gravity field coefficients used by the ICGEM (International Centre for Global Earth Models) described in the format description The ICGEM-format [4]. In this file, the coefficients and the corresponding variances are stored. Additionally to this file we provide a full covariance matrix of the coefficients in a separate file. This enables users to fully exploit the available information about the covariances of the estimated parameters. It also provides the possibility to compare our models to others in more detail. Due to the size of the full covariance matrices they are only provided upon request to the authors.

6 WP 4 - Comparison and Validation of computed gravity field models

6.1 Inputs

The inputs for this work package are mostly identical to the outputs of work package 3. This comprises the produced gravity field solutions and the corresponding variance information in terms of variances and also full covariance matrices.

6.2 Tasks

6.2.1 Comparison of gravity field solutions based on variances

The mostly used approach for validation of gravity field solutions is to compare a model to another on the basis of square-root degree variances or square-root degree variances of coefficient differences. Square-root degree variances of coefficients are defined by the following relation

$$\sigma_n = \sqrt{\sum_{m=0}^{n} \left(C_{nm}^2 + S_{nm}^2 \right)} \,. \tag{6.1}$$

Similar to this relation also square-root degree error variances based on the estimated variances of the coefficients can be computed

$$\hat{\sigma}_n = \sqrt{\sum_{m=0}^{n} \left(\sigma_{C_{nm}}^2 + \sigma_{S_{nm}}^2 \right)} \,. \tag{6.2}$$

A third possibility is to compute the differences between the coefficients of two different gravity field models. If a model with a significantly higher accuracy is available it can serve as a reference or virtually the “true gravity field”. First step is to compute the differences between corresponding coefficients

$$\Delta C_{nm} = C_{nm}^{(1)} - C_{nm}^{(2)} \quad \text{and} \quad \Delta S_{nm} = S_{nm}^{(1)} - S_{nm}^{(2)} \,. \tag{6.3}$$

These differences are now used to compute square-root degree variances similar to equation 6.1, except that the coefficients are replaced by the differences.
To make square-root degree variances or square-root degree error variances more interpretable they can be displayed in terms of geoid heights

$$\sigma_n(N) = R \cdot \sigma_n \,. \tag{6.4}$$

The computed square-root degree variances are now displayed in a logarithmic plot and can be interpreted visually. An example of a degree variance plot can be seen in figure 31.

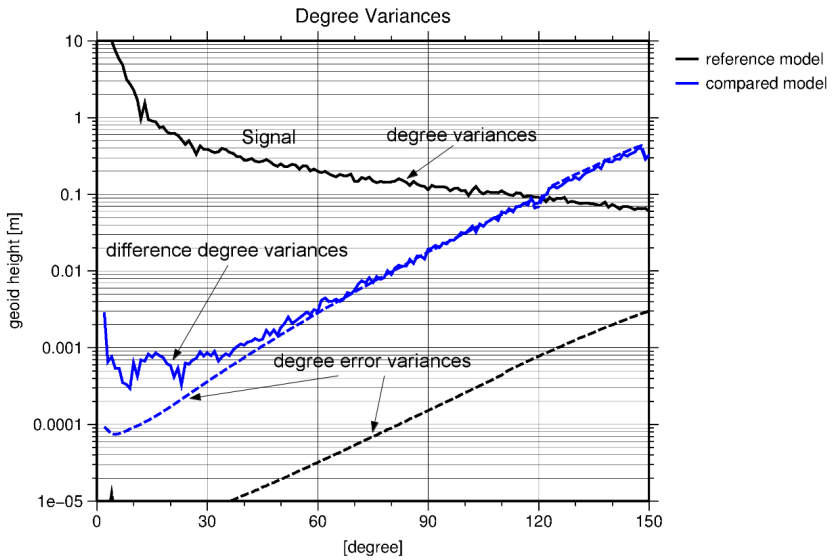

Figure 20: Example of a degree variance plot.

The degree variances described above are all defined as variance per degree. To interpret the over all accuracy of the gravity field solution up to a certain degree the separate degree error variances must be summed up to a certain degree and order

$$\sigma_N = \sqrt{\sum_{n=0}^{N} \sigma_n^2}\,. \tag{6.5}$$

From this definition it can be seen at which degree a certain accuracy level is reached. Degrees in turn can be interpreted as spatial resolution of the gravity field. If for example the accumulated degree error variance is 1 cm for a degree of 50, this means that the solution represents a gravity field with a spatial resolution of 400 km with an accuracy of 1 cm.
In case of solutions based on GOCE data a special aspect has to be considered. Due to the fact that the GOCE satellite flies in a sun synchronous orbit with an inclination of ~96,5° it never crosses the polar regions. Therefore no observations are available for these areas and the accuracy of gravity field estimations for these regions is bad. In case of the spherical harmonics expansion this means that the zonal and near zonal coefficients are estimated with a worse accuracy. This gets obvious when looking at the spherical harmonics triangles in figure 26. This circumstance also affects the computation of degree variances. To enable a comparison with other gravity field estimates the zonal and near zonal coefficients are excluded from degree variances according to the rule of *van Gelderen and Koop* [28]

$$m_{max} \approx \left| \frac{\pi}{2} - I \right| \cdot n \tag{6.6}$$

with I the inclination of the satellite's orbit in radians. This rule was applied for all computed degree variances throughout the whole project whenever GOCE data was involved or a comparison with a GOCE solution is made. As polar gap size 7°, respectively an inclination

of 97°, is chosen, because the orbit inclination is not exactly 96.5° and varies slightly with time.

CHAMP only model

Based on the available CHAMP data set covering a time span of January 1, 2002 till December 31, 2009, a CHAMP only gravity field was produced. In the following chapters this solution will be named ITSG-CHAMP. Some of the key parameters and data sets used in the estimation process are listed in Table 10 respectively Table 9. The used background models are described in chapter 5.1 Inputs.

Data	Time span	Sampling	Description
Precise orbit	01.01.2002 – 31.12.2002 01.01.2003 – 31.12.2009	30 s 10 s	Precise orbit positions provided by the AIUB
Satellite attitude	01.01.2002 – 31.12.2009	10 s	Attitude of the satellite derived from star camera observations provided by the ISDC, data gaps were filled with simulated data
Non-gravitational acceleration	01.01.2002 – 31.12.2009	10	Non-conservative accelerations acting on the satellite observed by the on-board accelerometer provided by the ISDC, data gaps are filled with zeros

Table 9: Used CHAMP data sets.

Parameter	Value	Description
Reference field	GOCO02S D/O 150	Reference field to reduce observations to simplify the estimation process
Earth rotation	ITRF2010	Earth Rotation parameter following the IERS convention 2010
Min degree	2	Minimum degree of the estimated gravity field
Max degree	120	Maximum degree of the estimated gravity field
GM	3.986004415e+14	Gravitational constant multiplied with earth mass
R	6378136.3 m	Mean earth radius
Interpolation degree	8	Degree of used polynomial for numerical differentiation
Used Epochs	9	Number of used epochs for numerical differentiation
Accelerometer Bias	1	Estimate an accelerometer bias in terms of a polynomial per arc with a certain degree

Table 10: Main parameters for gravity field estimation based on CHAMP data.

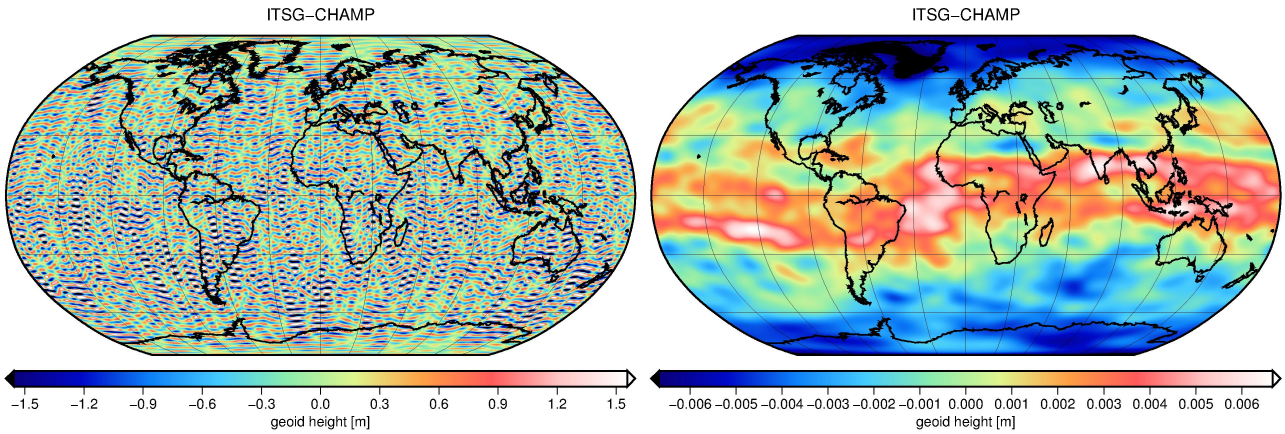

Figure 21: Difference of ITSG-CHAMP with respect to GOCO02S up to degree and order 120 in terms of geoid height. Unfiltered (left) and with Gaussian filter (radius 500km) filtered solution (right).

Figure 21 shows the difference in terms of geoid height between the gravity field solution ITSG-CHAMP and the GOCO02S model up to degree and order 120. The left plot shows unfiltered geoid heights. In contrast, for the right plot the geoid heights have been filtered in the spatial domain with a 500 km Gaussian filter. The unfiltered differences show a pretty regular distribution over the whole earth and an amplitude of approximately ± 1.5 m. But after filtering, the solution shows a strong positive deviation in the equatorial regions, possibly related to the earth's geomagnetic equator. But the amplitude of the differences reduces to ± 6 mm. As the GOCO02S model comprises more data from different satellite missions it can be seen as the reference or virtually the “truth” in this comparison. Therefore the conclusion from the above shown figures is, that the ITSG-CHAMP gravity field has an accuracy of ~1 cm with a spatial resolution of 500 km.

Figure 22 shows degree variances of the estimated gravity field ITSG-CHAMP in comparison to four state-of-the-art models.

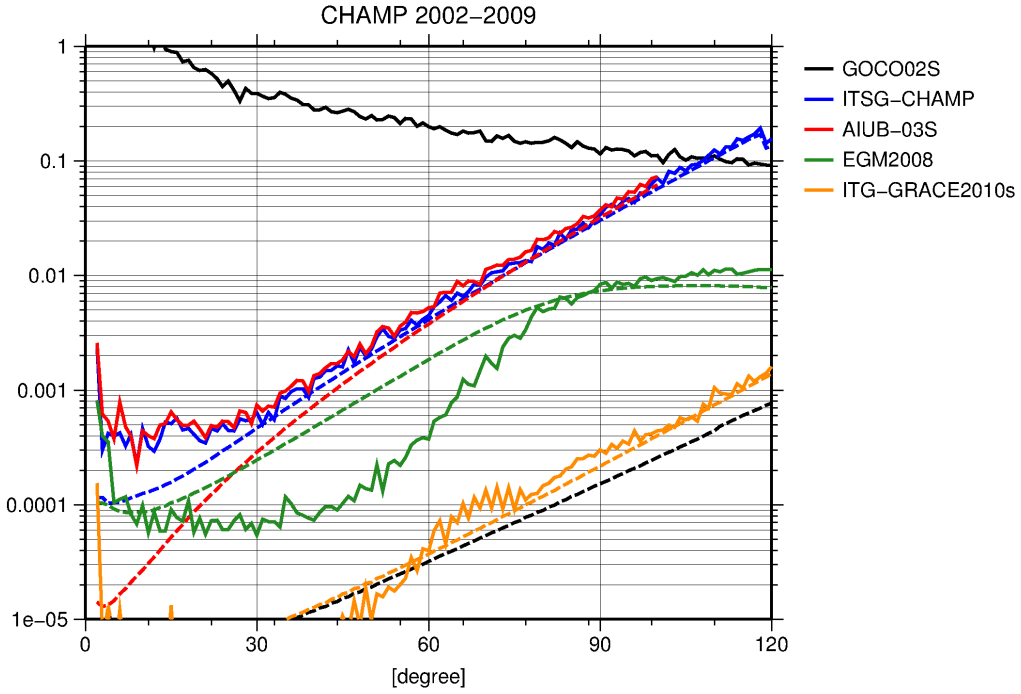

Figure 22: ITSG-CHAMP solution compared to GOCO02S, AIUB-03S, EGM2008 and ITG-GRACE2010s. The dotted lines show the formal errors of the corresponding model.

From figure 22 it can be seen, that the ITSG-CHAMP model performs pretty similar to the AIUB-03S model, but is highly outperformed by EGM2008 and ITG-GRACE2010s [18]. This can easily be explained by the fact that ITG-GRACE2010s is based on a long time series of GRACE data and EGM2008 contains the GRACE solution of ITG-GRACE03S. In comparison to GOCO02S it can be seen that the CHAMP-only model can reproduce the static gravity field up to a spherical harmonic degree of about 110. The similar performance of ITSG-CHAMP compared to AIUB-03S is due to the fact that they are based on the same orbit solution produced at the AIUB. The only difference between these two models is the way how the coefficients are estimated. At the University of Bern the so called celestial mechanics approach is used to estimate gravity fields from precise orbit information. In contrast to this, for producing the ITSG-CHAMP solution the acceleration approach has been used. This comparison shows that the acceleration approach can produce gravity field estimates with at least the same performance as the celestial mechanics approach and does not suffer from any inherent deficiencies.

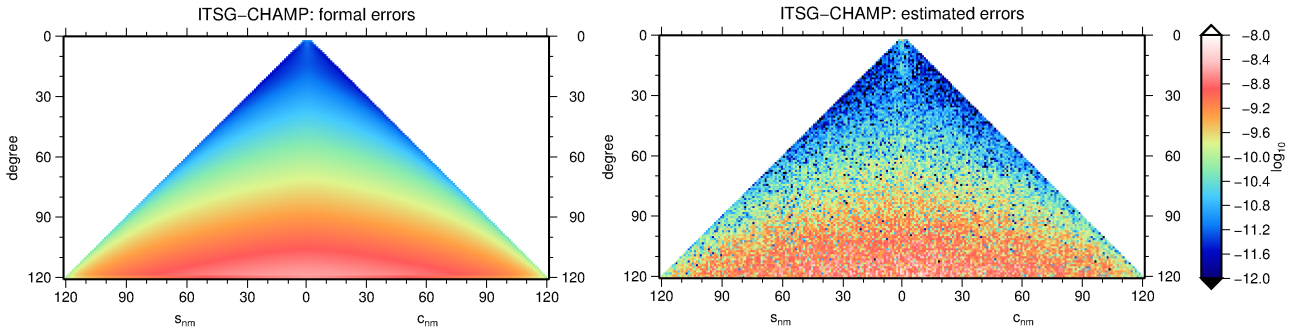

Figure 23: Spherical harmonics triangle of ITSG-CHAMP: formal errors (left) and differences of coefficients compared to GOCO02S (right).

Figure 23 shows on the left side the spherical harmonics triangle of ITSG-CHAMP formal errors. On the right side differences between ITSG-CHAMP and GOCO02S coefficients are plotted. In this comparison the GOCO02S model can be taken as a reference solution, because it features a much higher accuracy than the SST-hl CHAMP solution. The agreement between the two plots is quite good. This means, that the formal errors from the estimation process are a good indicator for the accuracy of the produced gravity field solution. This can also be seen from figure 22 were the formal errors match the degree variances quite well.

GOCE only model

For the GOCE satellite a data set spanning from 01. November 2009 till 31. August 2011 is available and was used to produce a SST-hl only gravity field solution. In the following chapters this solution will be named as ITSG-GOCE. The key parameters and data sets used in the estimation process are listed in Table 12 respectively Table 11. The used background models are the same as for the ITSG-CHAMP model already described in chapter 5.1 Inputs.

Data	Time span	Sampling	Description
Precise orbit	01.11.2009 – 31.07.2011	1 s	Precise orbit positions provided by the GOCE HPF Product: GO_CONS_SST_PSO
Satellite attitude	01.11.2009 – 31.07.2011	1 s	Attitude of the satellite derived from star camera observations Product: GO_CONS_EGG_IAQ
Non-gravitational acceleration	01.11.2009 – 31.07.2011	1	Non-conservative accelerations acting on the satellite observed by the satellite gradiometer in common mode. Product: GO_CONS_EGG_CCD

Table 11: Used GOCE data sets.

Parameter	Value	Description
Reference field	GOCO02S D/O 180	Reference field to reduce observations to simplify the estimation process
Earth rotation	ITRF2010	Earth Rotation parameter following the IERS convention 2010
Min degree	2	Minimum degree of the estimated gravity field
Max degree	150	Maximum degree of the estimated gravity field
GM	3.986004415e+14	Gravitational constant multiplied with earth mass
R	6378136.3 m	Mean earth radius
Interpolation degree	8	Degree of used polynomial for numerical differentiation
Used Epochs	9	Number of used epochs for numerical differentiation
Accelerometer Bias	1	Estimate an accelerometer bias in terms of a polynomial per arc with a certain degree

Table 12: Main parameters for gravity field estimation based on GOCE data.

Prior to the final estimation process different investigations were carried out concerning the used parameters. One test concentrated on the used sampling of the data set. The results for one month can be seen in figure 24. It shows solutions based on the original data set (blue) and reduced data sets (red and green). The degree variances for the 1 s and the 5 s sampled data sets are pretty similar. Only the solution based on 10 s sampled data performs worse in higher degrees. From this comparison it can be concluded that by reducing the original data set to a sampling of 5 s no information is lost.

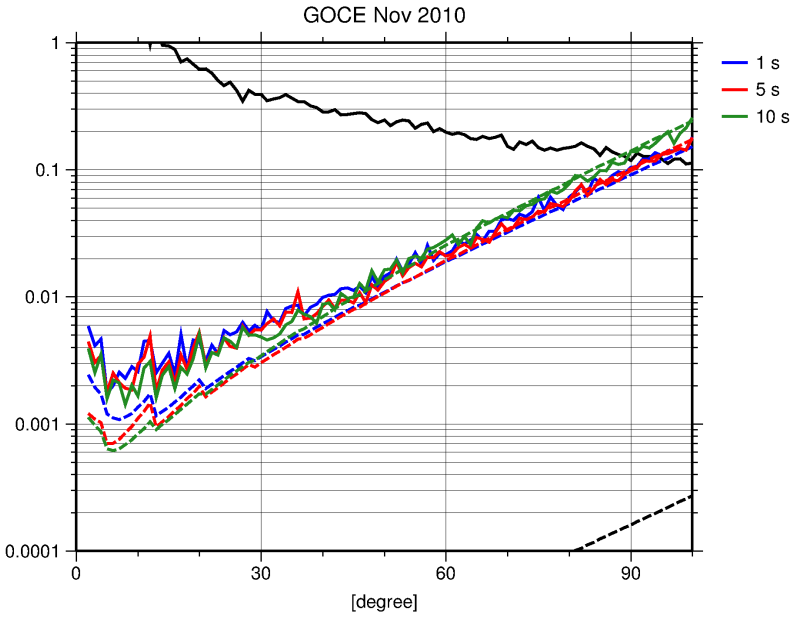

Figure 24: Degree variances of results for November 2010 based on data sets with a different sampling rate.

Therefore, the final estimation process was carried out with a reduced sampling of the data. The reduction was performed simply by taking every fifth epoch of the original data set.

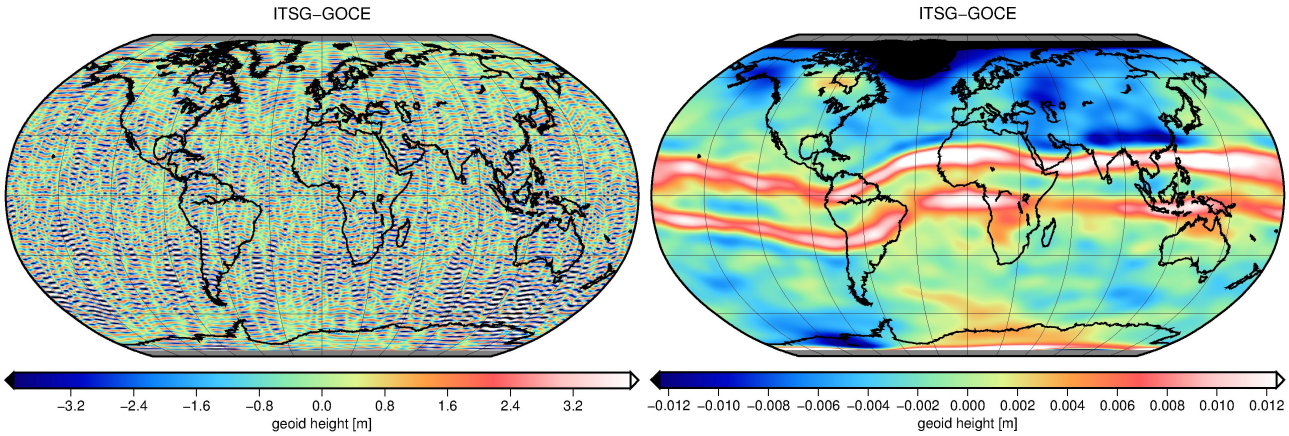

Figure 25: Difference of ITSG-GOCE with respect to GOCO02S up to degree and order 150 in terms of geoid height. Unfiltered (left) and with Gaussian filter (radius 500km) filtered solution (right).

The difference of ITSG-GOCE with respect to GOCO02S up to degree and order 150 is shown in terms of geoid height in figure 25. On the left hand side the differences are directly plotted. On the right hand side the differences are filtered with a Gaussian filter with a radius of 500 km to suppress the high frequency components. All in all, ITSG-GOCE performs comparable to ITSG-CHAMP. Only the amplitudes are higher in both plots. For the unfiltered differences this is due to the fact that the ITSG-GOCE model is estimated up to degree 150. Therefore the model contains more degrees were the noise exceeds the signal. The higher amplitude in the filtered differences can be explained by the fact that the ITSG-CHAMP model comprises more than twice the amount of data compared to the GOCE model. But the ITSG-GOCE model also shows the largest positive deviations in the equatorial region likely related to the earth's magnetic equator. This phenomenon must be investigated separately.

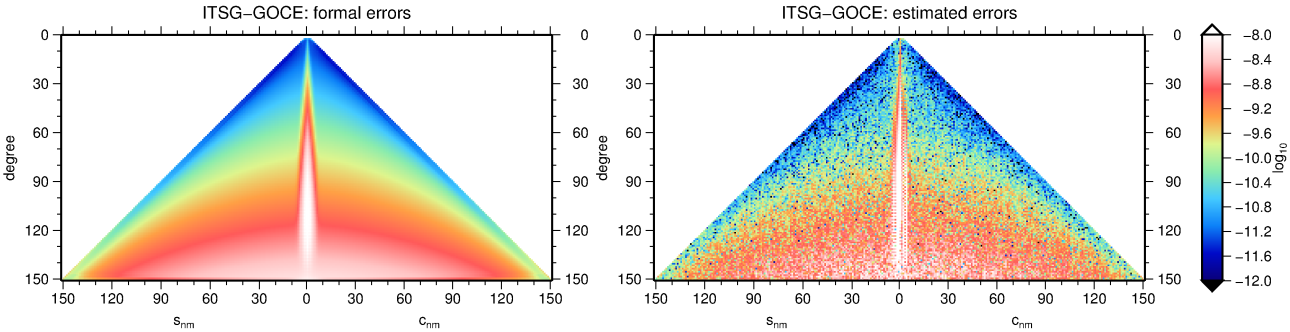

Figure 26: Spherical harmonics triangle of ITSG-GOCE: formal errors (left) and differences of coefficients compared to GOCO02S (right).

Figure 26 again shows the spherical harmonics triangle of the ITSG-GOCE solution compared to the GOCO02S model. When comparing the formal errors on the left side to the differences with respect to the GOCO02S model it shows that the formal errors give a quite good indication of the achieved accuracy. One big difference to the CHAMP model are the badly estimation of the zonal and near zonal coefficients. This fact can be ex-

plained by the fact that the GOCE satellite flies in a sun synchronous orbit with an inclination of 96°. Because of this orbit design the GOCE satellite never crosses the polar regions and therefore no observations are available for these areas. In the gravity field estimation process this affects the zonal and near zonal coefficients of the spherical harmonic expansion.

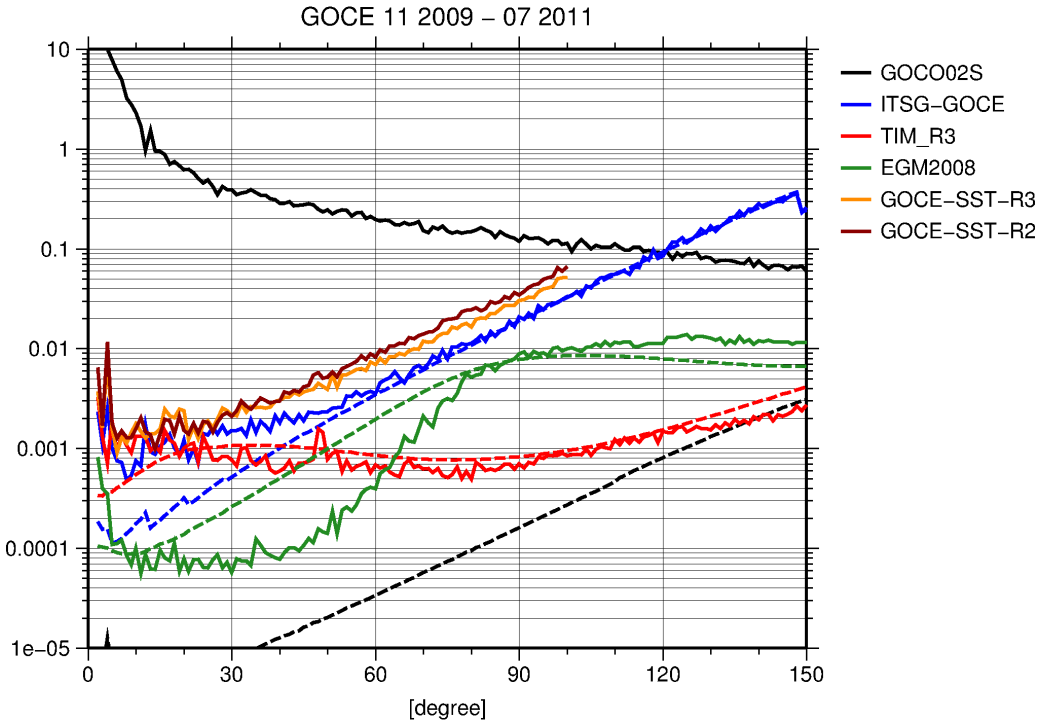

Figure 27: ITSG-GOCE solution compared to GOCO02S, TIM-R3, EGM2008 and the SST only parts of the official GOCE time-wise releases 2 and 3. The dotted lines show the formal errors of the corresponding model.

Figure 27 shows degree variances of the ITSG-GOCE solution compared to state-of-the-art gravity field models. Special attention must be given to the comparison with the GOCE SST only solutions used for the official time-wise releases 2 and 3. These two solutions are based on the same orbit data as the ITSG-GOCE solution. The release 3 solution is based on a data set spanning from November 1, 2009 till April 31, 2011. This time frame is only 3 months shorter than the one used for ITSG-GOCE. But the big difference between these two solutions and the ITSG-GOCE is the approach used in the estimation process. The official GOCE time-wise release is produced with the energy balance approach. For this method the orbit positions are used to compute the velocity of the satellite. These velocities are then used as observations. In contrast to the acceleration approach only one velocity is computed for each epoch. This reduces the available observations by factor of 3. This factor can now be seen in the resulting gravity field estimations. The degree variances of ITSG-GOCE are smaller by a factor of $\sqrt{3}$ than the GOCE-SST release 3. This relation holds for degrees 45 and higher. For lower degrees the solutions perform quite similar. This can be explained by the fact that the orbit positions still contain some systematic effects which degrade all three solutions.

Combined model GOCE-CHAMP

The above described models based on GOCE or CHAMP data have been produced by combining monthly solutions. The combination was carried out by putting together the normal equations of all months. The combination incorporated a variance component estimation to account for the different accuracies in different months. As all monthly normal equations are available it is easy to combine GOCE and CHAMP data. All in all 96 months of CHAMP data and 20 months of GOCE data have been combined to produce a combined solution based only on the SST-hl principle.

Figure 28 shows the combined solution compared to the GOCO02S model. When looking at the geoid height plots, ether the unfiltered or the filtered, it shows a pretty similar behavior as the CHAMP- or GOCE-only models. But when looking at the spherical harmonics triangle of the formal or the estimated errors, displayed in figure 30, it can be seen that the combination eliminates some deficiencies of the separate models. First of all the polar gap problem of the GOCE-only solution is removed, which can be seen in the errors of the zonal or near zonal coefficients. Secondly the low flying GOCE satellite improves the sectoral coefficients. All in all the combination features the best SST-hl only solution. The noise exceeds signal at approximately degree 120, which corresponds to a spatial resolution of ~160 km.

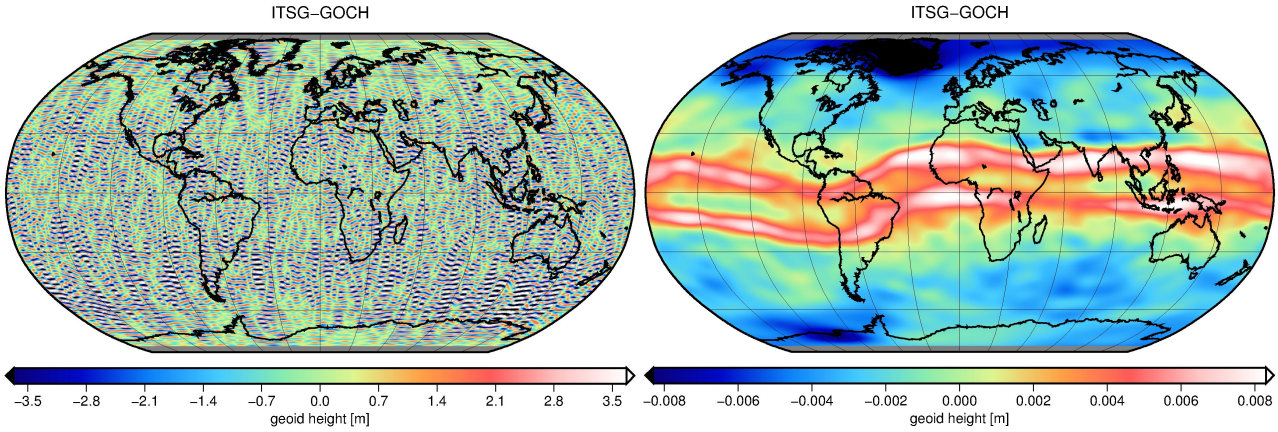

Figure 28: Difference of ITSG-GOCH with respect to GOCO02S up to degree and order 150 in terms of geoid height. Unfiltered (left) and with Gaussian filter (radius 500km) filtered solution (right).

From figure 29 it can be seen, that the noise exceeds signal at approximately degree 120, which corresponds to a spatial resolution of ~160 km. From the degree variances shown in figure 29 it can also be seen that ITSG-CHAMP and ITSG-GOCH solutions outperform the GOCE time-wise release 3 in the low degrees up to degree 30. One reason for this is the amount of used CHAMP data (96 months) compared to the GOCE data in the time-wise release (18 months). Another reason, already mentioned above, is the different approaches used in the estimation process.

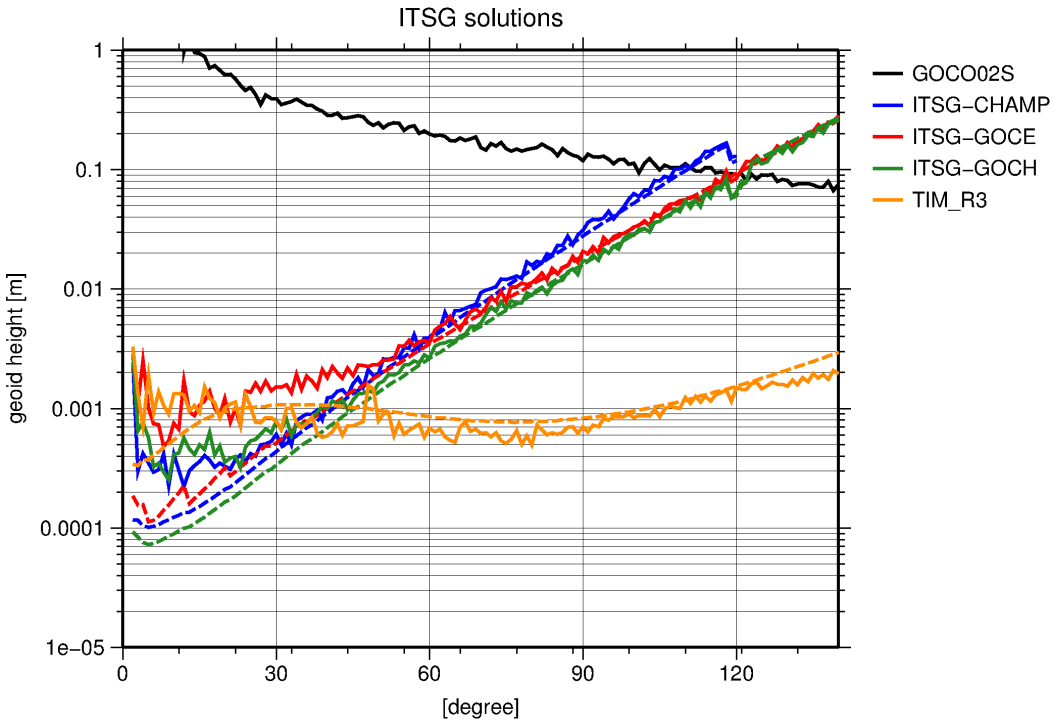

Figure 29: ITSG-GOCH solution compared to GOCO02S, ITSG-CHAMP, ITSG-GOCE and TIM-R3. The dotted lines show the formal errors of the corresponding model.

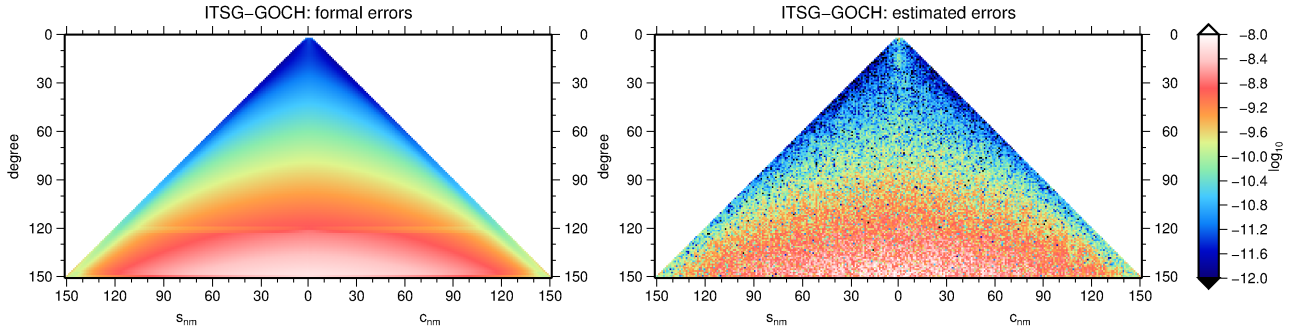

Figure 30: Spherical harmonics triangle of ITSG-GOCH: formal errors (left) and differences of coefficients compared to GOCO02S (right).

In figure 30 the spherical harmonics triangle of the combined CHAMP-GOCE solution is displayed. Comparison with the other two models reveals the advantage of combining different satellite mission. First of all it gets obvious that the included CHAMP data eliminates the deficiencies of the GOCE mission concerning the near zonal coefficients. Secondly due to the fact that more data is included the error of each coefficient is reduced. This leads to the assumption that the combined model features the best quality of the three different models.

6.2.2 Accumulated degree error variances

In contrast to the above used degree error variances, which only represent the variance of one degree, the values can be accumulated from minimum degree up to a certain degree. This accumulated degree variances then represent the error of a solution up to a certain degree. Figure 31 shows the accumulated degree error variances of the three ITSG solutions.

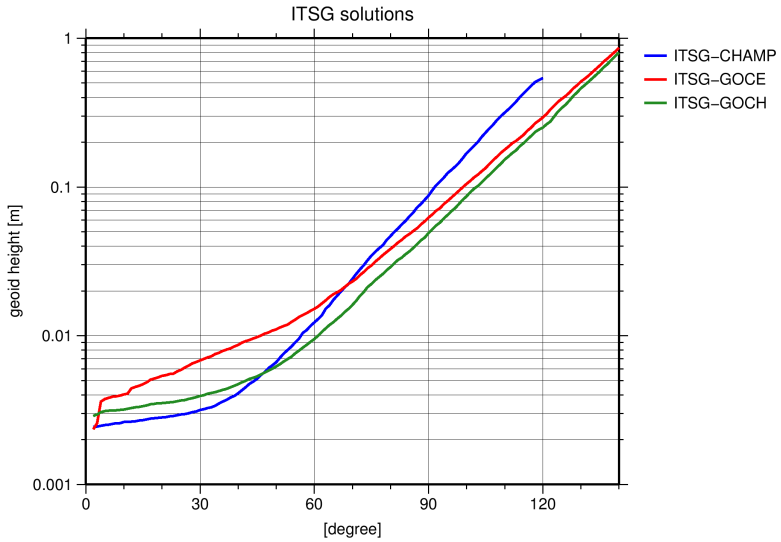

Figure 31: Accumulated degree error variances of the ITSG solutions.

When looking at the three graphs in detail the following values, listed in table 13, for certain accuracy levels can be found. Table 13 contains the degree and the corresponding spatial resolution at which certain accuracy levels are reached.

	Accuracy levels		
Solution	1 cm	2 cm	10 cm
ITSG-CHAMP	56 / 357 km	67 / 299 km	92 / 217 km
ITSG-GOCE	45 / 435 km	67 / 299 km	100 / 200 km
ITSG-GOCH	61 / 328 km	74 / 270 km	103 / 194 km
GOCE-TIM-SST-R3	15 / 1333 km	51 / 392 km	91 / 220 km
AIUB03S	55 / 364 km	66 / 303km	91 / 220 km

Table 13: Degree and spatial resolution of accumulated degree error variances at certain accuracy levels for the three ITSG solutions and the SST solution included in the GOCE time-wise release 3.

From this comparison it can be seen that the combined solution has an accuracy of 2 cm at a spatial resolution of 270 km. In comparison to that the SST solution used for the official GOCE time-wise release 3 only provides a spatial resolution of 392 km at the same accuracy level.

6.2.3 Omission and commission error

A special case of the above described accumulated degree error variance is the so-called commission error. It represents the accumulated degree error variance up to the maximum degree of the gravity field. The counter part of the commission error is the omission error. It represents the error introduced by omitting all signal components of higher degrees than

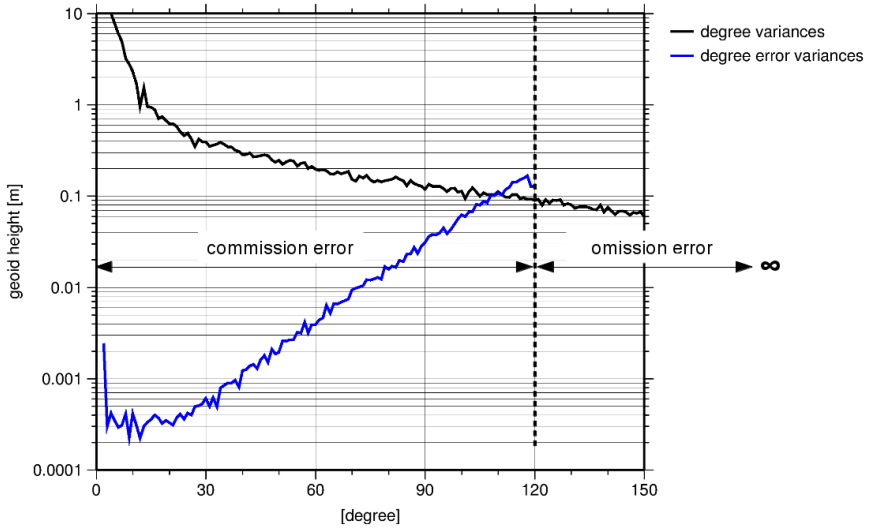

Figure 32: Illustration of commission and omission error.

included in the gravity field solution. The relationship is illustrated in figure 32.
Evaluating the commission and omission error for the three generated ITSG solutions the following values, listed in table Fehler: Referenz nicht gefunden, are generated.

Solution	Degree/Order	Commission error	Omission error
ITSG-GOCE	150	126,8 cm	~43 cm
ITSG-GOCH	150	121,0 cm	~43 cm
ITSG-CHAMP	120	53,7 cm	~54 cm
ITSG-GOCE	120	29,2 cm	~54 cm
ITSG-GOCH	120	25,1 cm	~54 cm

Table 14: Commission and omission error of the three ITSG gravity field solutions.

This comparison gives quite high values for the commission error, because the maximum degree and order for the solutions has been chosen high enough to fully exploit the whole signal included in the observations and to be prepared for additional observation data from the GOCE satellite. This will improve the accuracy and then also the coefficients of higher degrees will get estimable with sufficient accuracy. To get a fair comparison the three models are evaluated to a maximum degree and order of 120. This comparison then shows the best results for the combined model. Also striking is the fact that the CHAMP-only solution performs quite worse than the models with GOCE data included. This is due to the fact that the CHAMP satellite was flying in a higher orbit than the GOCE satellite, throughout its whole lifetime of ten years.

6.3 Outputs

The outputs of work package four are in general the results mentioned in chapter 6.2 Tasks. As this measures all together quantify the quality of the produced gravity field solutions. From these gained numerical values the following conclusions can be extracted:

- achieved accuracy: ~2 cm error in geoid height at a resolution of 270-300 km (~D/O 70)
- combined solution performs best
- unknown systematic effects related to the geomagnetic equator degrade the solutions in low degrees
- GOCE only solution outperforms the SST-hl component of the official GOCE timewise release
- CHAMP solution is equal or slightly better than AIUB03S

All in all the generated gravity field solutions are comparable to other solutions based on precise orbit positions using other methods, as for example the short arc integral method or the celestial mechanics approach.

7 Conclusions and Outlook

Briefly it can be said that in the frame of this project a software was implemented to estimated gravity fields from precise orbit information using the acceleration approach. This software is integrated in a very powerful tool which comprises different tasks in the frame of gravity field estimation, visualization and interpretation. All in all this enables the ITSG to perform varying tasks in the context of gravity field processing at a high scientific level.
In terms of real data application during the project various different gravity field estimates were produced. Three of them are now published and are available to other users for free. Comparison with other state-of-the-art models showed that the produced solutions can compete with others in terms of quality. In terms of quality information it can be said that the provided variance estimations showed very good agreement when compared to highly accurate reference gravity fields, like the GOCO02S.
As a long term goal the ITSG has set itself the vision of a consistent processing chain from pure GNSS observations to a gravity field estimation. This will incorporate tasks like determination of precise GNSS orbits and clock corrections as a basis for precise orbit determination of satellites like GOCE or CHAMP. This orbits are then used to generate the gravity field estimations. The fact that this whole processing chain will be carried out at the same institution and with the same software will minimize the discrepancies in terms of used models, parametrization and further more. This work flow can be optimized which then would enable the ITSG to gain the maximum benefit from the available data sets and in turn produce the optimal gravity field solutions. In the context of this long term goal the present project ACAP was another important step towards this goal.

References

[1]: **Austen G., Reubelt T.**, Räumliche Schwerefeldanalyse aus semi-kontinuierlichen Ephemeriden niedrigfliegender GPS-vermessener Satelliten vom Typ CHAMP, GRACE und GOCE, Geodätisches Institut der Universität Stuttgart, 2000, Stuttgart, Germany

[2]: **Badura T.**, Gravity Field Analysis from Satellite Orbit Information applying the Energy Integral Approach, Institute of Navigation and Satellite Geodesy/TU Graz, 2006, Graz, Austria

[3]: **Badura T., Sakulin C., Gruber C., Klostius R.**, Derivation of the CHAMP-only global gravity field model TUG-CHAMP04 applying the energy integral approach, , Institute of Geophysics of the Academy of Sciences of the Czech Republic, 2005, Czech Republic

[4] : **Barthelmes, F.; Förste, C.**, The ICGEM-format, 2011, GFZ Potsdam, Department 1 Geodesy and Remote Sensing, http://icgem.gfz-potsdam.de/ICGEM/

[5]: **Ditmar P., van Eck van der Sluijs A., Kuznetsov V.**, Modelling the Earth's gravity field from precise satellite orbit data: the acceleration approach works!, , Delft University of Technology, 2004, Delft, The Netherlands

[6]: **ESA**, CIGAR II: study on precise gravity field determination methods and mission requirements. Final report, ESA contract 7521/87/F/FL, European Space Agency, 1989, Noordwijk

[7]: **ESA**, CIGAR III/2: study on precise gravity field determination methods and mission requirements (phase 2). Final report, ESA contract 10713/93/F/FL, European Space Agency, 1995, Noordwijk

[8]: **ESA**, CIGAR III/1: study of the gravity field determination using gradiometry and GPS (phase 1). Final report, ESA contract 9877/92/F/FL, European Space Agency, 1993, Noordwijk

[9]: **Goiginger H.**, Gravity Field Processing based on GOCE Orbit Data, Institute of Navigation and Satellite Geodesy/TU Graz, 2008, Graz, Austria

[10]: **Goiginger H., Mayrhofer R., Heuberger F.** , Proposal: Global Gravity Field Modelling from Orbit Data based on the Acceleration Approach, Proposal, TU Graz, 2010, Graz, Austria

[11]: **Goiginger H., Rieser D., Mayer-Gürr T., Pail R., Fecher T., Gruber T., Albertella A., Maier A., Höck E., Krauss S., Hausleitner W., Baur O., Jäggi A., Meyer U., Brockmann J.M., Schuh W.-D., Krasbutter I., Kusche J.**, The combined satellite-only global gravity field model GOCO02S, Presented at the 2011 Gerneral Assembly of the European Geoscience Union,, , 2011, 4.-8. April, Vienna, Austria

[12]: **Hausleitner W., Kirchner G., Krauss S., Weingrill J., Pail R., Goiginger H., Rieser D.** Improved kHz-SLR tracking techniques and orbit quality analysis for LEO missions, Advances in Space Research, Vol. 45, Nr. 6, 2010, Elsevier, ISSN 0273-1177,

[13]: **Heiskanen W.A., Moritz H.**, Physical Geodesy, W.H. Freeman & Co Ltd ,1967, San Francisco, United States of America, ISBN: 978-0716702337

[14]: **Jandrisevits C.**, Numerische Differentiationsverfahren mit voller Kovarianzinformation im Rahmen der GOCE Erdschwerefeldlösung, Institute of Navigation and Satellite Geodesy/TU Graz, 2005, Graz, Austria

[15]: **Koch, K.R., Kusche, J.** Regularization of geopotential determination from satellite data by variance components, Journal of Geodesy, Vol. 76, Nr. , 2001, Springer, ,

[16]: **Koop R., Sünkel H., and the European GOCE Gravity Consortium**, GOCE: Preparation of the GOCE Level 1 to Level 2 Data Processing. Final report, ESA/ESTEC Contract No. 14986/01/NL/DC, European Space Agency, 2002, Noordwijk, The Netherlands

[17]: **Mayer-Gürr T.**, Gravitationsfeldbestimmung aus der Analyse kurzer Bahnbögen am Beispiel der Satellitenmissionen CHAMP und GRACE, Universität Bonn,2008, Bonn, Germany

[18]: **Mayer-Gürr, T.; Kurtenbach, E.; Eicker, A.**, ITG-GRACE2010 Gravity Field Model, ,2010, www.igg.uni-bonn.de/apmg/index.php?id=itg-grace2010

[19]: **Pail R.**, The Austrian Geoid 2007 (GEOnAUT), Final report, ASAP Phase III Project, ALR-OEWP-CO-329/06, , 2007, Graz, Austria

[20]: **Pail R.**, Gravity Field Processing Facility (GFPF) Graz, Final report, ASAP Phase II Project, ASAP-WV-211/05, , 2006, Graz, Austria

[21]: **Pail R.**, GOCE Data Archiving and Processing Center (DAPC) Graz, Final report, ASAP Bridging Phase Project, ASAP-CO-008/03, , 2004, Graz, Austria

[22]: **Pail R.**, GOCE Data Archiving and Processing Center (DAPC) Graz. Final report, ASAP Phase Ia Project, ASAP-CO-008/03, , 2003, Graz, Austria

[23]: **Pail R., Heuberger F., Rieser D., Gisinger C., Sharov A.**, Modelling snow-ice cover evolution and associated gravitational effects with GOCE constraints (ICEAGE), Final Report, , , 2010, Graz, Austria

[24]: **Pavlis, N.K.; Holmes, S.A.; Kenyon, S.C.; Factor**, An Earth Gravitational Model to Degree 2160: EGM2008, 2008, Vienna, European Geoscience Union General Assembly 2008

[25]: **Reubelt T.**, Harmonische Gravitationsfeldanalyse aus GPS-vermessenen kinematischen Bahnen niedrig fliegender Satelliten vom Typ CHAMP, GRACE und GOCE mit einem hoch auflösenden Beschleunigungsansatz , Geodätisches Institut der Universität Stuttgart,2009, Stuttgart, Germany

[26]: **Sünkel H.**, From Eötvös to mGal+. Final report, ESA/ESTEC Contract 14287/00/NL/DC, European Space Agency, 2002, Noordwijk, The Netherlands

[27]: **Sünkel H.**, From Eötvös to mGal. Final report, ESA/ESTEC Contract 13392/98/NL/GD, European Space Agency, 2000, Noordwijk, The Netherlands

[28]: **van Gelderen, M., Koop, R.** The use of degree variances in satellite gradiometry, Journal of Geodesy, Vol. 71, Nr. , 1997, Springer, ,

[29]: **Zehentner N., Mayrhofer R., Mayer-Gürr T.**, Gravitationsfeldbestimmung mittels Beschleunigungsansatz - Untersuchungen zur numerischen Differentiation, Presented at the Deutsche Geodätische Woche 2011,, Institute of Theoretical Geodesy and Satellite Geodesy , 2011, 27.-29. September, Nürnberg, Germany

[30]: **Zehentner, N., Mayer-Gürr, T., Mayrhofer, R.**, Gravity Field Determination using the Acceleration Approach - Considerations on Numerical Differentiation, Institute of Theoretical Geodesy and Satellite Geodesy,, , 2012, 23.-27.April, Vienna, European Geoscience Union, Gerneral Assembly 2012

[31]: , LAPACK routine dgorgqr, The University of Tennessee and The University of Tennessee Research Foundation, The University of California Berkeley, The University of Colorado Denver,2006, http://www.netlib.org/lapack/double/dorgqr.f

[32]: , LAPACK routine dgtrtri, The University of Tennessee and The University of Tennessee Research Foundation, The University of California Berkeley, The University of Colorado Denver,2006, http://www.netlib.org/lapack/double/dtrtri.f

[33]: , LAPACK routine dgeqrf, The University of Tennessee and The University of Tennessee Research Foundation, The University of California Berkeley, The University of Colorado Denver,2011, http://www.netlib.org/lapack/double/dgeqrf.f

[34]: , LAPACK routine dgetri, The University of Tennessee and The University of Tennessee Research Foundation, The University of California Berkeley, The University of Colorado Denver,2006, http://www.netlib.org/lapack/double/dgetri.f

[35]: , LAPACK routine dgetrf, The University of Tennessee and The University of Tennessee Research Foundation, The University of California Berkeley, The University of Colorado Denver,2006, http://www.netlib.org/lapack/double/dgetrf.f

[36]: , LAPACK routine dgesv, The University of Tennessee and The University of Tennessee Research Foundation, The University of California Berkeley, The University of Colorado Denver,2006, http://www.netlib.org/lapack/double/dgesv.f

[37]: , LAPACK, The University of Tennessee and The University of Tennessee Research Foundation, The University of California Berkeley, The University of Colorado Denver,2010, http://www.netlib.org/lapack/

List of abbreviations

ACAP	Global Gravity Field Modelling from Orbit Data based on the Acceleration Approach
AIUB	Astronomical Institute University of Bern
ASAP	Austrian Space Applications Program
CHAMP	Challenging Mini-satellite Payload
EGM2008	Earth Gravitational Model 2008
ESA	European Space Agency
FFG	Austrian Research Promotion Agency
GFZ	German Research Center for Geosciences
GOCE	Gravity Field and steady-state ocean circulation explorer
GOCO	Gravity Observation Combination
GPS	Global Positioning System
GRACE	Gravity Recovery and Climate Experiment
GROOPS	Gravity Recovery Object Oriented Programming System
HPF	High-level Processing Facility
INAS	Institute of Navigation
ISDC	Information System and Data Center
ITSG	Institute of Theoretical Geodesy and Satellite Geodesy
LAPACK	Linear Algebra Package
LEO	Low Earth Orbiter
POD	Precise Orbit Determination
PSD	Power spectral density
rms	Root mean square
SST-hl	Satellite-to-Satellite tracking in high-low mode

List of figures

List of tables